PHYSICAL REVIEW D **75,** 054004 (2007)

$B \to V\gamma$ beyond QCD factorization

Patricia Ball,* Gareth W. Jones,† and Roman Zwicky‡

IPPP, Department of Physics, University of Durham, Durham DH1 3LE, United Kingdom

(Received 14 December 2006; published 2 March 2007)

We calculate the main observables in $B_{u,d} \to (\rho, \omega, K^*)\gamma$ and $B_s \to (\bar{K}^*, \phi)\gamma$ decays, i.e. branching ratios and CP and isospin asymmetries. We include QCD factorization results and also the dominant contributions beyond QCD factorization, namely, long-distance photon emission and soft-gluon emission from quark loops. All contributions beyond QCD factorization are estimated from light-cone sum rules. We devise, in particular, a method for calculating soft-gluon emission, building on earlier ideas developed for analogous contributions in nonleptonic decays. Our results are relevant for new-physics searches at the B factories, CERN LHC and a future superflavor factory. Using current experimental data, we also extract $|V_{td}/V_{ts}|$ and the angle γ of the unitarity triangle. We give detailed tables of theoretical uncertainties of the relevant quantities which facilitates future determinations of these Cabibbo-Kobayashi-Maskawa parameters from updated experimental results.

DOI: 10.1103/PhysRevD.75.054004 PACS numbers: 12.39.St, 13.20.He

I. INTRODUCTION

The flavor-changing neutral-current (FCNC) transitions $b \to s\gamma$ and $b \to d\gamma$ are among the most valuable probes of flavor physics. Assuming the standard model (SM) to be valid, these processes offer the possibility to extract the Cabibbo-Kobayashi-Maskawa (CKM) matrix elements $|V_{t(d,s)}|$, in complementarity to, on the one hand, the determination from B mixing and, on the other hand, the SM unitarity triangle (UT) based on the tree-level observables $|V_{ub}/V_{cb}|$ and the angle γ. These decays are also characterized by their high sensitivity to new-physics (NP) contributions and by the particularly large impact of short-distance QCD corrections; see Ref. [1] for a review. Considerable time and effort have gone into the calculation of these corrections which are now approaching next-to-next-to-leading-order accuracy [2,3]. On the experimental side, both exclusive and inclusive $b \to s\gamma$ branching ratios are known with good accuracy, 5% for $B \to K^*\gamma$ and 7% for $B \to X_s\gamma$, while the situation is less favorable for $b \to d\gamma$ transitions: measurements are only available for exclusive channels. In Table I we give the branching ratios of all established exclusive $b \to (d, s)\gamma$ channels.

Whereas the inclusive modes can be computed perturbatively, using fixed-order heavy-quark expansion or soft-collinear effective theory (SCET) [2,7], the treatment of exclusive channels is more complicated. With presently available methods, it is impossible to simulate the full amplitude on the lattice, the reason being the occurrence of nonlocal correlation functions associated with the insertion of the electromagnetic interaction operator into the effective Hamiltonian for $b \to (s, d)\gamma$. Instead, one has to resort to effective field theory methods, which yield an expansion in inverse powers of the b quark mass, m_b. It was shown, in SCET, that the relevant hadronic matrix elements factorize to all orders in α_s and to leading order in $1/m_b$ and can be written as [8]

$$\langle V\gamma|Q_i|B\rangle = e^* \cdot \Bigg[T_1^{B\to V}(0) T_i^I + \int_0^1 d\xi du T_i^{II}(\xi, u)\phi_B(\xi)\phi_{2;V}^{\perp}(u) \Bigg] \times \{1 + O(1/m_b)\}. \quad (1)$$

This formula coincides with that obtained earlier in QCD factorization (QCDF) to next-to-leading order in α_s [9–14]. In (1), e_μ is the photon's polarization four-vector, Q_i is one of the operators in the effective Hamiltonian for $b \to (s, d)$ transitions, $T_1^{B\to V}$ is a $B \to V$ transition form factor, and ϕ_B, $\phi_{2;V}^{\perp}$ are leading-twist light-cone distribution amplitudes (DAs) of the B meson and the vector meson V, respectively. These quantities are universal nonperturbative objects and describe the long-distance dynamics of matrix elements, which is factorized from the perturbative short-distance interactions included in the hard-scattering kernels T_i^I and T_i^{II}. $B \to V\gamma$ decays have also been investigated in the alternative approach of perturbative QCD factorization (pQCD) [15].

Equation (1) is sufficient to calculate observables that are dominated by the leading-order term in the heavy-quark expansion, like $\mathcal{B}(B \to K^*\gamma)$. For $\mathcal{B}(B \to (\rho, \omega)\gamma)$, however, power-suppressed corrections play an important role, for instance, weak annihilation (WA) which is mediated by a tree-level diagram. In this case, the parametric suppression by one power of $1/m_b$ is alleviated by an enhancement factor $2\pi^2$ relative to the loop-suppressed contributions at leading order in $1/m_b$. Power-suppressed contributions also determine the time-dependent CP asymmetry in $B \to V\gamma$ (see Refs. [16–19]), as well as isospin asymmetries [20]—all observables with a potentially large contribution from NP. The purpose of this paper is to calculate the dominant power-suppressed contributions to

*Email address: Patricia.Ball@durham.ac.uk
†Email address: G.W.Jones@durham.ac.uk
‡Email address: Roman.Zwicky@durham.ac.uk

TABLE I. Experimental branching ratios of exclusive $b \to (d, s)\gamma$ transitions. All entries are CP averaged. The first error is statistical, the second systematic. $B \to (\rho, \omega)\gamma$ is the CP average of the isospin average over ρ and ω channels: $\bar{\mathcal{B}}(B \to (\rho, \omega)\gamma) = \frac{1}{2}\{\bar{\mathcal{B}}(B^\pm \to \rho^\pm\gamma) + \frac{\tau_{B^\pm}}{\tau_{B^0}} \times [\bar{\mathcal{B}}(B^0 \to \rho^0\gamma) + \bar{\mathcal{B}}(B^0 \to \omega\gamma)]\}$.

$\mathcal{B} \times 10^6$	*BABAR* [4]	Belle [5]	$\mathcal{B} \times 10^6$	HFAG [6]
$B \to (\rho, \omega)\gamma$	$1.25^{+0.25}_{-0.24} \pm 0.09$	$1.32^{+0.34+0.10}_{-0.31-0.09}$	$B^+ \to K^{*+}\gamma$	40.3 ± 2.6
$B^+ \to \rho^+\gamma$	$1.10^{+0.37}_{-0.33} \pm 0.09$	$0.55^{+0.42+0.09}_{-0.36-0.08}$	$B^0 \to K^{*0}\gamma$	40.1 ± 2.0
$B^0 \to \rho^0\gamma$	$0.79^{+0.22}_{-0.20} \pm 0.06$	$1.25^{+0.37+0.07}_{-0.33-0.06}$		
$B^0 \to \omega\gamma$	<0.78	$0.96^{+0.34+0.05}_{-0.27-0.10}$		

(1) and the resulting branching ratios and CP and isospin asymmetries, using the most up-to-date hadronic input parameters for form factors and light-cone DAs. Although $1/m_b$ effects are, in principle, accessible in SCET, the vast majority of studies in this framework only includes leading-order effects, the reason being a proliferation of new effective operators at power-suppressed accuracy (see Ref. [21]), whose matrix elements induce subleading form factors and are largely unknown. For this reason, in this paper we adopt a different approach not based on SCET and calculate power-suppressed corrections using the method of QCD sum rules on the light cone (LCSRs). The present paper is an extension of our previous work, Ref. [22], where we calculated the ratio of branching ratios $\mathcal{B}(B \to (\rho, \omega)\gamma)/\mathcal{B}(B \to K^*\gamma)$ in order to determine the ratio of CKM matrix elements $|V_{td}/V_{ts}|$ from data. Some of these power corrections, namely, those related to WA contributions and the isospin asymmetry in $B \to K^*\gamma$, have already been calculated in QCDF [12–14,20]. Other power corrections cannot be calculated in the framework of QCDF. The most relevant of these come from soft-gluon emission from quark loops and long-distance photon emission from soft quarks. We have already calculated some of these contributions before, using LCSRs: long-distance photon emission in Ref. [23] and soft-gluon emission from charm loops in Ref. [19], using heavy-quark expansion in powers of $1/m_c$. In this paper, we complete these calculations and develop a method to also calculate soft-gluon emission from light-quark loops, thus allowing us to predict branching ratios and isospin and CP asymmetries for exclusive $B \to V\gamma$ transitions with increased precision. We also include the B_s decays $B_s \to \phi\gamma$, which is a $b \to s\gamma$ transition, and $B_s \to K^*\gamma$, which is $b \to d\gamma$. All these decays will be studied in detail at CERN LHC, and those of $B_{u,d}$ at future superflavor factories [24].

Our paper is organized as follows: in Sec. II we introduce notations and recall QCDF formulas. In Sec. III we calculate the WA contributions and in Sec. IV the long-distance contributions to the $B \to V\gamma$ amplitude from heavy- and light-quark loops. In Sec. V we present results for branching ratios and asymmetries; we summarize and conclude in Sec. VI. The Appendix contains a discussion of the longitudinal and transverse decay constants of vector mesons.

II. FRAMEWORK AND BASIC FORMULAS

The effective Hamiltonian for $b \to D\gamma$ transitions, with $D = s, d$, reads

$$H_{\text{eff}} = \frac{G_F}{\sqrt{2}} \sum_{U=u,c} \lambda_U^{(D)} \Big[C_1 Q_1^U + C_2 Q_2^U + \sum_{i=3\ldots8} C_i Q_i \Big], \quad (2)$$

where $\lambda_U^{(D)} = V_{UD}^* V_{Ub}$. This Hamiltonian implicitly relies on the SM unitarity relation, also referred to as the Glashow-Iliopoulos-Maiani (GIM) mechanism,

$$\lambda_t^{(D)} + \lambda_c^{(D)} + \lambda_u^{(D)} = 0, \quad (3)$$

which enters the calculation of the penguin contributions. The operators are given by

$$\begin{aligned}
&Q_1^U = (\bar{D}_i U_j)_{V-A}(\bar{U}_j b_i)_{V-A}, \qquad Q_2^U = (\bar{D}U)_{V-A}(\bar{U}b)_{V-A}, \qquad Q_3 = (\bar{D}b)_{V-A}\sum_q (\bar{q}q)_{V-A}, \\
&Q_4 = (\bar{D}_i b_j)_{V-A}\sum_q (\bar{q}_j q_i)_{V-A}, \qquad Q_5 = (\bar{D}b)_{V-A}\sum_q (\bar{q}q)_{V+A}, \qquad Q_6 = (\bar{D}_i b_j)_{V-A}\sum_q (\bar{q}_j q_i)_{V+A}, \\
&Q_7 = \frac{e}{8\pi^2} m_b \bar{D}\sigma^{\mu\nu}(1+\gamma_5)F_{\mu\nu}b + \frac{e}{8\pi^2} m_D \bar{D}\sigma^{\mu\nu}(1-\gamma_5)F_{\mu\nu}b, \\
&Q_8 = \frac{g}{8\pi^2} m_b \bar{D}\sigma^{\mu\nu}(1+\gamma_5)G_{\mu\nu}b + \frac{g}{8\pi^2} m_D \bar{D}\sigma^{\mu\nu}(1-\gamma_5)G_{\mu\nu}b,
\end{aligned} \quad (4)$$

where $(\bar{q}Q)_{V-A}(\bar{r}R)_{V\pm A} \equiv (\bar{q}\gamma_\mu(1-\gamma_5)Q)(\bar{r}\gamma^\mu(1\pm\gamma_5)R)$. The sign conventions for the electromagnetic and strong couplings correspond to the covariant derivative $D_\mu = \partial_\mu + ieQ_f A_\mu + igT^a A_\mu^a$. With these definitions the coefficients $C_{7,8}$ are negative in the SM, which is the choice generally adopted in the literature. The above operator basis, which we

shall label BBL after the authors of Ref. [25], is the same as that of Ref. [12], except that Q_1 and Q_2 are exchanged. For some applications, in particular, calculations of inclusive $b \to D\gamma$ transitions, a different operator basis proves more suitable: the basis adopted, for instance, in Refs. [26,27], labeled CMM in the following, has $Q_{7(8)}^{\rm CMM} = Q_{7(8)}^{\rm BBL}$, but differs in $Q_{1\ldots6}$. It turns out that we need the Wilson coefficients in both bases:

(i) $C_{1\ldots6}^{\rm BBL}(\mu \sim m_b)$, calculated according to Ref. [25], for power-suppressed (WA and soft-gluon emission) contributions;

(ii) $C_{1\ldots8}^{\rm CMM}(\mu \sim m_b)$, calculated according to Ref. [26], for hard-vertex corrections in QCDF which are given in terms of two-loop matrix elements for $b \to D\gamma$ transitions obtained in Ref. [27], in the CMM basis;

(iii) $C_{1\ldots6}^{\rm BBL}(\mu \sim 2\ {\rm GeV})$ and $C_8^{\rm CMM}(\mu \sim 2\ {\rm GeV})$ for hard-spectator corrections in QCDF; although these coefficients refer to a different basis, it is correct to use them together as the corresponding operators $Q_{7,8}$ are identical in both bases and independent of the basis chosen for the four-quark operators.

Numerical values of all C_i are given in Table II. Note that the question of whether to use Wilson coefficients (and other scale-dependent hadronic quantities) at LO or NLO accuracy is actually nontrivial. Strictly speaking, NLO accuracy is mandatory only for C_7, as only for this term is the hadronic matrix element also known to NLO accuracy (see below). We will evaluate all $O(\alpha_s)$ and power-suppressed corrections using both LO and NLO scaling for Wilson coefficients and hadronic matrix elements and include the resulting discrepancies in the theoretical uncertainty.

The calculation of the decay amplitudes of exclusive $B \to V\gamma$ decays also requires the knowledge of hadronic matrix elements of type $\langle V\gamma|Q_i|B\rangle$. A complete calculation of these quantities is not possible to date, but the leading term in an expansion in $1/m_b$ is obtained from QCDF; see Eq. (1). The factorization formula is valid in the heavy-quark limit $m_b \to \infty$ and is subject to corrections of order $\Lambda_{\rm QCD}/m_b$. Some of these corrections are numerically very relevant: for instance, the contributions from all operators but Q_2 are loop suppressed; hence, the tree-level WA diagram in Fig. 1, which is suppressed by one power of m_b, comes with a relative enhancement factor $\sim 4\pi^2$. This contribution, with the operator Q_2, is doubly Cabibbo suppressed for $b \to s\gamma$ transitions, but carries no CKM suppression factor in $b \to d\gamma$ transitions. WA can also be induced by the penguin operators $Q_{3\ldots6}$ and in this case carries no CKM suppression in $b \to s\gamma$, but comes with small (loop-suppressed) Wilson coefficients. Other examples for relevant power-suppressed corrections are CP and isospin asymmetries, Refs. [16,19,20], which actually vanish in the heavy-quark limit. This indicates that in $B \to V\gamma$ transitions simple $1/m_b$ counting is, in general, not sufficient to determine the numerical relevance of a particular contribution, but that all relevant factors,

(i) order of power suppression in $1/m_b$,

(ii) loop suppression or tree enhancement,

(iii) CKM suppression,

(iv) size of hadronic matrix elements,

have to be taken into account. This is a consequence of the fact that in radiative transitions the ''naively'' leading term

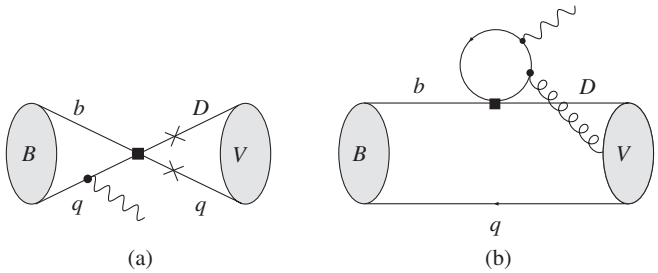

FIG. 1. (a): WA diagram. The square denotes insertion of the operator Q_i. Photon emission from lines other than the B spectator is power suppressed, except for emission from the final-state quark lines for the operators $Q_{5,6}$, denoted by crosses. (b): soft-gluon emission from a quark loop. Again the square dot denotes the insertion of the operator Q_i. There is also a second diagram where the soft gluon is picked up by the B meson.

TABLE II. NLO Wilson coefficients to be used in this paper, at the scales $m_b = 4.2$ GeV and $\mu_h = 2.2$ GeV. The coefficients labeled BBL correspond to the operator basis of Ref. [25] and given in Eq. (4), whereas CMM denotes the basis of Ref. [26]. We use $\alpha_s(m_Z) = 0.1176$ [28] and $m_t(m_t) = 163.6$ GeV [29]. Note that $C_1^{\rm BBL}$ and $C_2^{\rm BBL}$ are exchanged with respect to the basis of Ref. [12] and that $C_{7(8)}^{\rm BBL} = C_{7(8)}^{\rm CMM}$; see text. Following [13], the CMM set is used for calculating hard-vertex corrections to the QCDF formulas and the BBL set at the lower scale μ_h is used to calculate hard-spectator corrections. The BBL set at scale m_b is used for the calculation of power corrections.

$C_1^{\rm CMM}(m_b)$	$C_2^{\rm CMM}(m_b)$	$C_3^{\rm CMM}(m_b)$	$C_4^{\rm CMM}(m_b)$	$C_5^{\rm CMM}(m_b)$	$C_6^{\rm CMM}(m_b)$	$C_7^{\rm CMM}(m_b)$
-0.322	1.009	-0.005	-0.874	0.0004	-0.001	-0.309
$C_1^{\rm BBL}(m_b)$	$C_2^{\rm BBL}(m_b)$	$C_3^{\rm BBL}(m_b)$	$C_4^{\rm BBL}(m_b)$	$C_5^{\rm BBL}(m_b)$	$C_6^{\rm BBL}(m_b)$	$C_8^{\rm CMM}(m_b)$
-0.189	1.081	0.014	-0.036	0.009	-0.042	-0.170
$C_1^{\rm BBL}(\mu_h)$	$C_2^{\rm BBL}(\mu_h)$	$C_3^{\rm BBL}(\mu_h)$	$C_4^{\rm BBL}(\mu_h)$	$C_5^{\rm BBL}(\mu_h)$	$C_6^{\rm BBL}(\mu_h)$	$C_8^{\rm CMM}(\mu_h)$
-0.288	1.133	0.021	-0.051	0.010	-0.065	-0.191

in Q_7 is loop suppressed, which is qualitatively different from other applications of QCDF, for instance in $B^- \to \pi^-\pi^0$, where the leading hadronic matrix element describes a tree-level process.

The exclusive $B \to V\gamma$ process is actually described by two physical amplitudes, one for each polarization of the photon:

$$\begin{aligned}\bar{\mathcal{A}}_{L(R)} &= \mathcal{A}(\bar{B} \to V\gamma_{L(R)}),\\ \mathcal{A}_{L(R)} &= \mathcal{A}(B \to \bar{V}\gamma_{L(R)}),\end{aligned} \tag{5}$$

where $\bar{B}$ denotes a $(b\bar{q})$ and V a $(D\bar{q})$ bound state.[1] In the notation introduced in Ref. [12] in the context of QCDF, the decay amplitudes can be written as

$$\begin{aligned}\bar{\mathcal{A}}_{L(R)} &= \frac{G_F}{\sqrt{2}}(\lambda_u^D a_7^u(V\gamma_{L(R)}) + \lambda_c^D a_7^c(V\gamma_{L(R)}))\langle V\gamma_{L(R)}|Q_7^{L(R)}|\bar{B}\rangle \equiv \frac{G_F}{\sqrt{2}}(\lambda_u^D a_{7L(R)}^u(V) + \lambda_c^D a_{7L(R)}^c(V))\langle V\gamma_{L(R)}|Q_7^{L(R)}|\bar{B}\rangle,\\ \mathcal{A}_{L(R)} &= \frac{G_F}{\sqrt{2}}((\lambda_u^D)^* a_{7R(L)}^u(V) + (\lambda_c^D)^* a_{7R(L)}^c(V))\langle \bar{V}\gamma_{L(R)}|(Q_7^{R(L)})^\dagger|B\rangle.\end{aligned} \tag{6}$$

The $a_7^{c,u}$ calculated in Refs. [12,13] coincide, to leading order in $1/m_b$, with our a_{7L}^U, whereas a_{7R}^U are set to zero in [12,13]. Our expression (6) is purely formal and does not imply that the $a_{7R(L)}^U$ factorize at order $1/m_b$. As a matter of fact, they do not. The operators $Q_7^{L(R)}$ are given by

$$Q_7^{L(R)} = \frac{e}{8\pi^2} m_b \bar{D}\sigma_{\mu\nu}(1 \pm \gamma_5) b F^{\mu\nu}$$

and generate left- (right-)handed photons in the decay $b \to D\gamma$. The matrix elements in (6) can be expressed in terms of the form factor $T_1^{B\to V}$ as

$$\begin{aligned}\langle V(p,\eta)\gamma_{L(R)}(q,e)|Q_7^{L(R)}|\bar{B}\rangle &= -\frac{e}{2\pi^2} m_b T_1^{B\to V}(0)[\epsilon^{\mu\nu\rho\sigma} e_\mu^* \eta_\nu^* p_\rho q_\sigma \pm i\{(e^*\eta^*)(pq) - (e^*p)(\eta^*q)\}]\\ &\equiv -\frac{e}{2\pi^2} m_b T_1^{B\to V}(0) S_{L(R)},\\ \langle \bar{V}(p,\eta)\gamma_{L(R)}(q,e)|(Q_7^{R(L)})^\dagger|B\rangle &= -\frac{e}{2\pi^2} m_b T_1^{B\to V}(0) S_{L(R)},\end{aligned} \tag{7}$$

where $S_{L,R}$ are the helicity amplitudes corresponding to left- and right-handed photons, respectively, and $e_\mu(\eta_\mu)$ is the polarization four-vector of the photon (vector meson). The definition of $T_1^{B\to V}$ can be found in Ref. [36]; our convention for the epsilon tensor follows that of Bjorken & Drell: $\mathrm{Tr}[\gamma^\alpha\gamma^\beta\gamma^\gamma\gamma^\delta\gamma_5] = 4i\epsilon^{\alpha\beta\gamma\delta}$. Up-to-date values for all decays studied in this paper are given in Table III. The nonperturbative parameters are taken from experiment, where available, from lattice (f_B), from QCD sum rules ($a_i^\perp$) and from QCD sum rules on the light cone (T_1); for the decay constants $f^\perp$, results are available from both lattice and QCD sum rules; they are discussed in the Appendix. No lattice results are available for $a_i^\perp$ and only partial results for T_1 [46]. The numbers in Table III differ slightly from those given in Ref. [36] because we include updates of the hadronic input parameters. We do not include isospin breaking in the form factors since it is caused by the difference of quark masses and electric charges and expected to be of the order of 1% only. This is indeed the size of isospin breaking in the form factor indicated by recent measurements of $D^0 \to (K^-, \pi^-)e^+\nu$ and $D^+ \to (\bar{K}^0, \pi^0)e^+\nu$ at CLEO [47]. At this point we would also like to comment on the UT angle γ. The value given in Table III comes from Belle's Dalitz-plot analysis of the CP asymmetry in $B^- \to (K_S^0\pi^+\pi^-)K^-$, with $K_S^0\pi^+\pi^-$ being a three-body final state common to both D^0 and $\bar{D}^0$. This method to measure γ from a new-physics–free tree-level process was suggested in Ref. [48] and has been implemented by both *BABAR* [49] and Belle [40], but the *BABAR* result currently suffers from huge errors. Other determinations of γ from QCDF or SCET analyses, or SU(3) or U-spin fits of nonleptonic B decays, or global UT fits, all come with theoretical uncertainties and/or possible contamination by unresolved new physics, so we decide to stick, as a reference point, to the tree-level result of Belle. For all observables with a pronounced dependence on γ, i.e. $b \to d\gamma$ branching ratios and isospin asymmetries, we will present results as a function of γ.

[1] Note that in this paper K^* is an $(s\bar{q})$ bound state, in contrast to the standard labeling, according to which $K^{*0} = (d\bar{s})$ and $\bar{K}^{*0} = (s\bar{d})$. This is because the calculation of form factors and other matrix elements involves light-cone DAs of the vector meson V, and in the standard notation used in that context, K^* always contains an s quark and $\bar{K}^*$ an $\bar{s}$ quark. This distinction is relevant because of a sign change of G-odd matrix elements under $(s\bar{q}) \leftrightarrow (q\bar{s})$; see Tables III, V, and VI.

TABLE III. Summary of input parameters. The value of $|V_{ub}|$ is our own average over inclusive and exclusive determinations and the result from UT angles; see Refs. [6,30,31]. None of our results is very sensitive to $|V_{ub}|$. For an explanation of our choice of the value of the UT angle γ, see text. λ_B is the first inverse moment of the B meson's light-cone DA. λ_{B_s} is obtained from λ_{B_q} as described in the text. The vector-meson decay constants f_V, $f_V^\perp$ are discussed in the Appendix; the values of the Gegenbauer moments $a_i^\perp$ are compiled from various sources [22,32–34] and include only small SU(3) breaking, in line with the findings for pseudoscalar mesons [35]. The form factors T_1 are obtained from LCSRs and are updates of our previous results [36], including the updated values of the decay constants $f_{\rho,\omega,\phi}$ and of $a_1^\perp(K^*)$ [37,38]. Note that $a_1^\perp(K^*)$ refers to an $(s\bar{q})$ bound state; for a $(q\bar{s})$ state it changes sign. All scale-dependent quantities are given at the scale $\mu = 1$ GeV unless stated otherwise.

CKM parameters and couplings					
λ [28]	$\lvert V_{cb}\rvert$ [39]	$\lvert V_{ub}\rvert$	γ [40]	$\alpha_s(m_Z)$ [28]	α
0.227(1)	$42.0(7) \times 10^{-3}$	$4.0(7) \times 10^{-3}$	$(53 \pm 20)°$	0.1176(20)	1/137
B parameters					
f_{B_q} [41]	f_{B_s} [41]	$\lambda_{B_q}(\mu_h)$ [22]	$\lambda_{B_s}(\mu_h)$	μ_h	
200(25) MeV	240(30) MeV	0.51(12) GeV	0.6(2) GeV	2.2 GeV	
ρ parameters					
f_ρ	$f_\rho^\perp$	$a_1^\perp(\rho)$	$a_2^\perp(\rho)$	$T_1^{B\to\rho}(0)$	
216(3) MeV	165(9) MeV	0	0.15(7)	0.27(4)	
ω parameters					
f_ω	$f_\omega^\perp$	$a_1^\perp(\omega)$	$a_2^\perp(\omega)$	$T_1^{B\to\omega}(0)$	
187(5) MeV	151(9) MeV	0	0.15(7)	0.25(4)	
K^* parameters					
f_{K^*}	$f_{K^*}^\perp$	$a_1^\perp(K^*)$ [37]	$a_2^\perp(K^*)$	$T_1^{B_q\to K^*}(0)$	$T_1^{B_s\to\bar{K}^*}(0)$
220(5) MeV	185(10) MeV	0.04(3)	0.15(10)	0.31(4)	0.29(4)
ϕ parameters					
f_ϕ	$f_\phi^\perp$	$a_1^\perp(\phi)$	$a_2^\perp(\phi)$	$T_1^{B_s\to\phi}(0)$	
215(5) MeV	186(9) MeV	0	0.2(2)	0.31(4)	
Quark masses					
$m_s(2\text{ GeV})$ [42]	$m_b(m_b)$ [39]	$m_c(m_c)$ [43]	$m_t(m_t)$ [29]		
100(20) MeV	4.20(4) GeV	1.30(2) GeV	163.6(2.0) GeV		

As for the a_7 coefficients, the $a_{7L}^{c,u}(V)$ are, in QCDF, of order 1 in a $1/m_b$ expansion,

$$a_{7L}^{c,u}(V) = C_7 + O(\alpha_s, 1/m_b), \tag{8}$$

whereas $a_{7R}^{c,u}(V)$ are of order $1/m_b$ [17,18]. It proves convenient to split these coefficients into three contributions which we will investigate separately:

$$\begin{aligned} a_{7L}^{U}(V) &= a_{7L}^{U,\mathrm{QCDF}}(V) + a_{7L}^{U,\mathrm{ann}}(V) + a_{7L}^{U,\mathrm{soft}}(V) + \ldots, \\ a_{7R}^{U}(V) &= a_{7R}^{U,\mathrm{QCDF}}(V) + a_{7R}^{U,\mathrm{ann}}(V) + a_{7R}^{U,\mathrm{soft}}(V) + \ldots, \end{aligned} \tag{9}$$

where $a_{7L}^{U,\mathrm{QCDF}}$ is the leading term in the $1/m_b$ expansion; all other terms are suppressed by at least one power of m_b. We only include those power-suppressed terms that are either numerically large or relevant for isospin and CP asymmetries. The dots denote terms of higher order in α_s and further $1/m_b$ corrections to QCDF, most of which are incalculable. Explicit formulas for $a_{7L}^{U,\mathrm{QCDF}}$, complete to $O(\alpha_s)$, can be found in Ref. [13]. $a_{7L}^{U,\mathrm{ann}}$ encodes the $O(1/m_b)$ contribution of the WA diagram of Fig. 1 which drives the isospin asymmetries and has been calculated, in QCDF, and to leading order in α_s, in Refs. [13,20] for ρ and K^*, and in Ref. [14] for ω. Preliminary results for the $O(\alpha_s)$ corrections to WA in $B \to \rho\gamma$ were presented in Ref. [50]. This contribution is also relevant for the branching ratio of $B \to (\rho, \omega)\gamma$; in this case, long-distance photon emission from the soft B spectator quark, which is $O(1/m_b^2)$, also becomes relevant and has been calculated in Refs. [23,51]. We discuss the WA contributions in Sec. III. The last terms in (9), $a_{7L(R)}^{U,\mathrm{soft}}$, encode soft-gluon emission from a (light or heavy quark) loop as shown in Fig. 1 and are particularly relevant for the CP asymmetry; they will be discussed in Sec. IV. In Ref. [20] another class of $1/m_b$ corrections to $B \to K^*\gamma$ was also calculated, namely, $O(\alpha_s)$ corrections to the isospin asymmetry in this decay. As these corrections break factorization (that is, they require an infrared cutoff in the momentum distribution of the valence quarks in the K^* meson) and are numerically small, we do not include them in our analysis. As for a_{7R}^{U}, the dominant contributions to $a_{7R}^{c}(K^*)$ were calculated in Ref. [19]. Here we extend this analysis to

other vector mesons and also develop a method to include light-quark loops.

We conclude this section by providing explicit results for the QCDF contributions to a_7, using the formulas of Ref. [13] and the Wilson coefficients and hadronic input parameters collected in Tables II and III. The decay constants f_V and $f_V^\perp$ are defined as

$$\begin{aligned}\langle 0|\bar{q}\gamma_\mu D|V(p)\rangle &= m_V f_V \eta_\mu,\\ \langle 0|\bar{q}\sigma_{\mu\nu} D|V(p)\rangle &= i(\eta_\mu p_\nu - p_\mu \eta_\nu) f_V^\perp;\end{aligned} \tag{10}$$

their numerical values are discussed in the Appendix. The other parameters in Table III pertaining to vector mesons are $a_1^\perp$ and $a_2^\perp$, the first and second Gegenbauer moments of their transversal light-cone DAs of leading twist. In this paper we do not want to go into any detail about light-cone DAs, their conformal expansion in Gegenbauer polynomials and the dependence of the Gegenbauer moments on the renormalization scale, but simply refer to the relevant literature [32–34].

It turns out that, at the level of two significant digits, all $a_{7L}^{c,\mathrm{QCDF}}$ are equal and so are the $a_{7L}^{u,\mathrm{QCDF}}$. For central values of the input parameters of Table III, we obtain

$$\begin{aligned}a_{7L}^{c,\mathrm{QCDF}}(V) &= -(0.41 + 0.03i) - (0.01 + 0.01i),\\ a_{7L}^{u,\mathrm{QCDF}}(V) &= -(0.45 + 0.07i) + (0.02 - 0i).\end{aligned} \tag{11}$$

Here we have split the result into contributions from vertex corrections (first term) and hard-spectator interactions (second term). The size of the hard-spectator corrections is set by the factor

$$h_V = \frac{2\pi^2}{9}\,\frac{f_B f_V^\perp}{m_B T_1^{B\to V}(0)\lambda_B}. \tag{12}$$

Note that our value of λ_{B_s}, the first inverse moment of the twist-2 B-meson light-cone DA, is obtained from that of λ_{B_d} by a simple scaling argument:

$$\frac{m_{B_s}}{\lambda_{B_s}}(\Lambda_{\mathrm{QCD}} + m_s) = \frac{m_{B_q}}{\lambda_{B_q}}\Lambda_{\mathrm{QCD}},$$

which follows from the assumption that the B_q DA peaks at the spectator momentum $k_+ = \Lambda_{\mathrm{QCD}}$, whereas that of B_s peaks at $\Lambda_{\mathrm{QCD}} + m_s$.

The parameters $a_{7R}^{U,\mathrm{QCDF}}$, at tree level, were obtained in Ref. [19] and read

$$a_{7R}^{U,\mathrm{QCDF}}(K^*,\phi) = C_7\frac{m_s}{m_b}, \qquad a_{7R}^{U,\mathrm{QCDF}}(\rho,\omega,\bar{K}^*) = C_7\frac{m_d}{m_b}. \tag{13}$$

III. WEAK ANNIHILATION CONTRIBUTIONS

The intrinsic WA diagram is shown in Fig. 1; the weak interaction operator is one of the charged-current or QCD-penguin operators. All these contributions are $O(1/m_b)$; photon emission from the b quark and the quarks in the vector meson is further suppressed and $O(1/m_b^2)$—unless the weak interaction operator is $Q_{5,6}$, which can be Fierz transformed into $(\bar{D}(1+\gamma_5)q)(\bar{q}(1-\gamma_5)b)$ and picks up an additional factor m_B from the projection onto the B meson DA which results in this contribution being $O(1/m_b)$. In Table IV we show the relative weights of these diagrams in terms of CKM factors and Wilson coefficients. The numerically largest contribution occurs for $B^\pm \to \rho^\pm\gamma$: it comes with the large combination of Wilson coefficients $C_2 + C_1/3 = 1.02$ and is not CKM suppressed. For $B^0 \to (\rho^0,\omega)\gamma$ it comes with the factor $C_1 + C_2/3 = 0.17$ instead and an additional suppression factor $1/2$ from the electric charge of the spectator quark (d instead of u). For all other decays, WA is suppressed by small (penguin) Wilson coefficients. We evaluate the annihilation diagrams at the scale $\mu = m_b$. Apart from $B \to (\rho,\omega)\gamma$, WA is not relevant so much for the total values of a_{7L}, but rather for isospin breaking, which is set by photon emission from the spectator quark. WA is the only mechanism to contribute to isospin asymmetries at tree level; see Ref. [20] for $O(\alpha_s)$ contributions.

Formulas for $a_{7L}^{U,\mathrm{ann}}(\rho, K^*)$ in QCDF can be found in Refs. [13,14]; in this approximation, there is no contribution to $a_{7R}^{U,\mathrm{ann}}$. In QCDF, the $a_{7L}^{U,\mathrm{ann}}$ are expressed in terms of the hadronic quantities

$$\begin{aligned}b^V &= \frac{2\pi^2}{T_1^{B\to V}(0)}\,\frac{f_B m_V f_V}{m_B m_b \lambda_B},\\ d_v^V &= -\frac{4\pi^2}{T_1^{B\to V}(0)}\,\frac{f_B f_V^\perp}{m_B m_b}\int_0^1 dv\,\frac{\phi_{2;V}^\perp(v)}{v}\end{aligned} \tag{14}$$

and $d_{\bar{v}}^V$, obtained by replacing $1/v \to 1/\bar{v}$ in the integrand; $\phi_{2;V}^\perp$ is the twist-2 DA of a transversely polarized vector meson. For B_s decays one has to set $f_B \to f_{B_s}$ and correspondingly for the other B meson parameters. Numerically, one finds, for instance for the ρ, $b^\rho = 0.22$ and $d^\rho = -0.59$, at the scale $\mu = 4.2$ GeV. As $T_1 \sim 1/m_b^{3/2}$ and $f_B \sim m_b^{-1/2}$ in the heavy-quark limit, these terms are $O(1/m_b)$, but not numerically small because of the tree-enhancement factors of π^2.

TABLE IV. Parametric size of WA contributions to $B \to V\gamma$. C denotes the charged-current operators $Q_{1,2}$, P the penguin operators $Q_{3,4,5,6}$; their Wilson coefficients are small (see Table II). CKM denotes the order in the Wolfenstein parameter λ with respect to the dominant amplitude induced by Q_7.

WA	$B^- \to K^{*-}$	$\bar{B}^0 \to K^{*0}$	$B \to (\rho,\omega)$	$B_s \to \phi$	$B_s \to \bar{K}^*$
Induced by	C (and P)	P	C and P	P	P
CKM	λ^2 (and 1)	1	1	1	1

For ω, $\bar{K}^*$, and ϕ we obtain

$$\begin{aligned}
a_{7L}^{u,\mathrm{ann}}(\omega)|_{\mathrm{QCDF}} &= Q_d b^{\omega}(a_1 + 2(a_3 + a_5) + a_4) \\
&\quad + Q_d(d_v^{\omega} + d_{\bar{v}}^{\omega})a_6, \\
a_{7L}^{c,\mathrm{ann}}(\omega)|_{\mathrm{QCDF}} &= Q_d b^{\omega}(2(a_3 + a_5) + a_4) \\
&\quad + Q_d(d_v^{\omega} + d_{\bar{v}}^{\omega})a_6, \\
a_{7L}^{U,\mathrm{ann}}(\phi)|_{\mathrm{QCDF}} &= Q_s b^{\phi}(a_3 + a_5) + Q_s(d_v^{\phi} + d_{\bar{v}}^{\phi})a_6, \\
a_{7L}^{U,\mathrm{ann}}(\bar{K}^*)|_{\mathrm{QCDF}} &= Q_s b^{\bar{K}^*} a_4 + Q_s(d_v^{\bar{K}^*} Q_d/Q_s + d_{\bar{v}}^{\bar{K}^*})a_6,
\end{aligned} \tag{15}$$

with $a_1 = C_1 + C_2/3$, $a_3 = C_3 + C_4/3$, $a_4 = C_4 + C_3/3$, $a_5 = C_5 + C_6/3$, $a_6 = C_6 + C_5/3$; note that $a_1 \leftrightarrow a_2$ as compared to [13], as in our operator basis (i.e. the BBL basis) Q_1 and Q_2 are exchanged. The expressions for ϕ and $\bar{K}^*$ are new; for ω, we do not agree with [14]. For completeness, we also give the annihilation coefficients for the ρ, K^*, and ω, as obtained in Ref. [13]:

$$\begin{aligned}
a_{7L}^{u,\mathrm{ann}}(K^{*0})|_{\mathrm{QCDF}} &= Q_d[a_4 b^{K^*} + a_6(d_v^{K^*} + d_{\bar{v}}^{K^*})], \\
a_{7L}^{u,\mathrm{ann}}(K^{*-})|_{\mathrm{QCDF}} &= Q_u[a_2 b^{K^*} + a_4 b^{K^*} \\
&\quad + a_6(Q_s/Q_u d_v^{K^*} + d_{\bar{v}}^{K^*})], \\
a_{7L}^{u,\mathrm{ann}}(\rho^0)|_{\mathrm{QCDF}} &= Q_d[-a_1 b^{\rho} + a_4 b^{\rho} + a_6(d_v^{\rho} + d_{\bar{v}}^{\rho})], \\
a_{7L}^{u,\mathrm{ann}}(\rho^-)|_{\mathrm{QCDF}} &= Q_u[a_2 b^{\rho} + a_4 b^{\rho} + a_6(Q_d/Q_u d_v^{\rho} + d_{\bar{v}}^{\rho})], \\
a_{7L}^{c,\mathrm{ann}}(K^{*0})|_{\mathrm{QCDF}} &= Q_d[a_4 b^{K^*} + a_6(d_v^{K^*} + d_{\bar{v}}^{K^*})], \\
a_{7L}^{c,\mathrm{ann}}(K^{*-})|_{\mathrm{QCDF}} &= Q_u[a_4 b^{K^*} + a_6(Q_s/Q_u d_v^{K^*} + d_{\bar{v}}^{K^*})], \\
a_{7L}^{c,\mathrm{ann}}(\rho^0)|_{\mathrm{QCDF}} &= Q_d[a_4 b^{\rho} + a_6(d_v^{\rho} + d_{\bar{v}}^{\rho})], \\
a_{7L}^{c,\mathrm{ann}}(\rho^-)|_{\mathrm{QCDF}} &= Q_u[a_4 b^{\rho} + a_6(Q_d/Q_u d_v^{\rho} + d_{\bar{v}}^{\rho})].
\end{aligned} \tag{16}$$

Apart from ρ and ω, all these coefficients are numerically small and do not change the branching ratio significantly; the terms in a_6, however, are relevant for the isospin asymmetries.

In view of the large size of $a_{7L}^{u,\mathrm{ann}}(\rho)$ it is appropriate to have a look at further corrections. The most obvious ones are $O(\alpha_s)$ corrections to the QCDF expressions, shown in Fig. 2. As it turns out, the corrections to the B vertex in Fig. 2(a) are known: they also enter the decay $B \to \gamma\ell\nu$ and were calculated in Ref. [52]. Numerically, they are at the level of 10%. Figure 2(b) shows the vertex corrections to the V vertex, which are actually included in the decay constant f_V. For the nonfactorizable corrections shown in Fig. 2(c), preliminary results have been reported in Ref. [50]; according to [50], these corrections are of a size similar to the B vertex corrections. Another class of corrections is suppressed by one power of m_b with respect to the QCDF contributions and is due to long-distance photon emission from the soft B spectator quark. A first calculation of this effect was attempted in Ref. [51] and was corrected and extended in Ref. [23]. The long-distance photon emission from a soft-quark line requires the inclusion of higher-twist terms in the expansion of the quark propagator in a photon background field, beyond the leading-twist (perturbative) contribution; a comprehensive discussion of this topic can be found in Ref. [53]. The quantity calculated in Ref. [23] is

$$\begin{aligned}
&\langle \rho^-(p)\gamma(q)|(\bar{d}u)_{V-A}(\bar{u}b)_{V-A}|B^-(p+q)\rangle \\
&\quad = e\frac{m_\rho f_\rho}{m_B}\eta_\mu^*\{F_V \epsilon^{\mu\nu\rho\sigma} e_\nu^* p_\rho q_\sigma - iF_A[e^{*\mu}(pq) \\
&\qquad - q^\mu(e^* p)]\} \\
&\quad = -e\frac{m_\rho f_\rho}{m_B}\left\{\frac{1}{2}F_V(S_L + S_R) + \frac{1}{2}F_A(S_L - S_R)\right\}
\end{aligned} \tag{17}$$

in terms of the photon-helicity amplitudes $S_{L,R}$. The above relation differs from the one given in [23] by an overall sign, which is due to the different convention used in [23] (and in [53]) for the covariant derivative: $D_\mu = \partial_\mu - ieQ_f A_\mu$ instead of $D_\mu = \partial_\mu + ieQ_f A_\mu$ as in this paper. In QCDF, $F_{A,V}$ are given by $Q_u f_B/\lambda_B$ and induce a term $Q_u a_2 b^{\rho}$ in $a_{7L}^{u,\mathrm{ann}}(\rho^-)$. The long-distance photon contribution to $F_{V,A}$ was found to be [23]

$$\begin{aligned}
F_A^{\mathrm{soft}} &= -0.07 \pm 0.02 \equiv Q_u G_A, \\
F_V^{\mathrm{soft}} &= -0.09 \pm 0.02 \equiv Q_u G_V,
\end{aligned} \tag{18}$$

with $G_A + G_V = -0.24 \pm 0.06$ and $G_V - G_A = -0.030 \pm 0.015$. Again, there is a relative sign with respect to the results in [23]. This comes from the fact that the product $eF_{A,V}^{\mathrm{soft}}$ is independent of the sign convention for e, and as we have changed the overall sign of (17) with respect to [23], we also have to change the sign of $F_{A,V}^{\mathrm{soft}}$. Stated differently, the relative sign between $F_{A,V}^{\mathrm{soft}}$ and $F_{A,V}^{\mathrm{hard}}$ in [23] is wrong because of a mismatch in sign conventions for e in the covariant derivative.

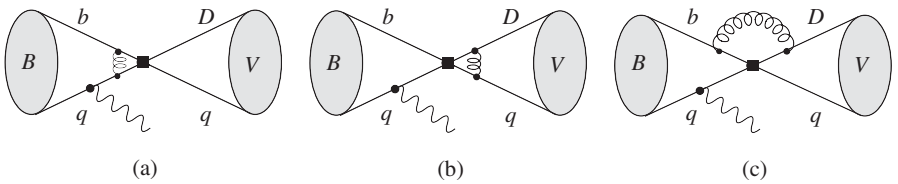

FIG. 2. Example radiative corrections to weak annihilation. The corrections to the B vertex in (a) are known [52] and those to the V vertex in (b) are included in f_V. For the nonfactorizable corrections in (c), only preliminary results are available (see text).

In order to obtain concise expressions for $a_{7L(R)}^{U,\mathrm{ann}}$, it proves convenient to define one more hadronic quantity:

$$g_{L,R}^{\rho} = \frac{\pi^2}{T_1^{\rho}} \frac{m_\rho f_\rho}{m_b m_B} (G_V \pm G_A) \tag{19}$$

and correspondingly for other mesons. g_L is $O(1/m_b^2)$ as $G_V + G_A$ has the same power scaling in m_b as T_1, i.e. $\sim m_b^{-3/2}$, as one can read off from the explicit expressions in [51]. The difference $G_V - G_A$, on the other hand, is a twist-3 effect due to three-particle light-cone DAs of the photon and is suppressed by one more power of m_b, i.e. $g_R \sim 1/m_b^3$. This quantity will enter the CP asymmetry. Our final expressions for $a_{7L(R)}^{U,\mathrm{ann}}$ then read

$$\begin{aligned} a_{7L}^{U,\mathrm{ann}}(V) &= a_{7L}^{U,\mathrm{ann}}(V)|_{\mathrm{QCDF}}(b^V \to b^V + g_L^V), \\ a_{7R}^{U,\mathrm{ann}}(V) &= a_{7L}^{U,\mathrm{ann}}(V)|_{\mathrm{QCDF}}(b^V \to g_R^V, d^V \to 0). \end{aligned} \tag{20}$$

Numerically, one has $g_L^\rho/b^\rho = -0.3$, so these corrections, despite being suppressed by one more power in $1/m_b$, are not small numerically and are larger than the known $O(\alpha_s)$ corrections to QCDF from $B \to \gamma \ell \nu$. Based on this, we feel justified in including these long-distance corrections in our analysis, while dropping the radiative ones of Figs. 2(a) and 2(c).

We conclude this section by listing the numerical values of some of the annihilation coefficients, for central values of the input parameters, including, in particular, those to which $Q_{1,2}$ contribute (with no Cabibbo suppression):

$$\begin{aligned} a_{7L}^{c,\mathrm{ann}}(K^{*0}) &= -0.013 - 0.001 \text{ LD}, \\ a_{7L}^{c,\mathrm{ann}}(K^{*-}) &= 0.004 + 0.001 \text{ LD}, \\ a_{7L}^{u,\mathrm{ann}}(\rho^0) &= -0.001 - 0.004 \text{ LD}, \\ a_{7L}^{u,\mathrm{ann}}(\rho^-) &= 0.149 - 0.043 \text{ LD}, \\ a_{7L}^{u,\mathrm{ann}}(\omega) &= -0.024 + 0.003 \text{ LD}. \end{aligned} \tag{21}$$

The contribution from the long-distance photon emission is labeled "LD" (LD $\to 1$ at the end). The unexpectedly small $a_{7L}^{u,\mathrm{ann}}(\rho^0)$ is due to a numerical cancellation between the charged-current and penguin-operator contributions. Comparing these results with those from QCDF, Eq. (11), it is evident that WA is, as expected, largely irrelevant for the branching ratios, except for $B^\pm \to \rho^\pm \gamma$.

IV. LONG-DISTANCE CONTRIBUTIONS FROM QUARK LOOPS

In this section we calculate the soft-gluon emission from quark loops shown in Fig. 1. Again, these contributions are suppressed by one power of m_b with respect to $a_{7L}^{U,\mathrm{QCDF}}$, but they also induce a right-handed photon amplitude which is of the same order in $1/m_b$ as $a_{7R}^{U,\mathrm{QCDF}}$. As we shall see in the next section, this amplitude induces the time-dependent CP asymmetry in $B \to V\gamma$. The asymmetry is expected to be very small in the SM and $\propto m_D/m_b$ due to chiral suppression of the leading transition, but could be drastically enhanced by NP contributions. It was noticed in Refs. [17,18] that the chiral suppression is relaxed by emission of a gluon from the quark loop, which is the topic of this section. The task is then not so much to calculate these contributions to high accuracy, but to exclude the possibility of *large* contributions to the CP asymmetry. For this reason we will be very generous with the theoretical uncertainties of the results obtained in this section—which are currently unavoidable due to the uncertainties of the relevant hadronic input parameters.

Historically, soft-gluon emission from a charm loop was first considered in Ref. [54] as a potentially relevant long-distance contribution to the branching ratio of $B \to K^*\gamma$, at about the same time as similar effects were being discussed for its inclusive counterpart $B \to X_s\gamma$ [55–57]. It was pointed out later, in Ref. [18], that the same diagram also contributes dominantly to the time-dependent CP asymmetry in $B^0 \to K^{*0}\gamma$. The size of this contribution was calculated only very recently, in Ref. [19]. The method used in [19] relies on the local operator-product expansion (OPE) of a heavy-quark loop in inverse powers of the quark mass and hence cannot be used to calculate soft-gluon emission from light-quark loops, which are doubly Cabibbo suppressed for $b \to s\gamma$ transitions, but not for $b \to d\gamma$. In Sec. IV A we will briefly review the results for heavy-quark loops and in Sec. IV B we will present a new technique for calculating light-quark loops; however, before we do so, we would like to fix our notation and give explicit expressions for $a_{7L(R)}^{U,\mathrm{soft}}$.

Potentially the most important contribution to the soft-gluon emission diagram in Fig. 1 comes from the charged-current operator Q_2^U with the large Wilson coefficient $C_2 \sim 1$; it vanishes for Q_1^U by gauge invariance. In order to calculate the diagram, it proves convenient to decompose Q_2^U by a Fierz transformation into

$$\begin{aligned} Q_2^U &= \frac{1}{3} Q_1^U + 2\tilde{Q}_1^U \quad \text{with} \\ \tilde{Q}_1^U &= \left(\bar{U} \frac{\lambda_a}{2} U\right)_{V-A} \left(\bar{D} \frac{\lambda_a}{2} b\right)_{V-A}. \end{aligned} \tag{22}$$

The contribution of the U-quark loop to the $\bar{B} \to V\gamma$ amplitude can then be written as

$$\begin{aligned} \mathcal{A}(\bar{B} \to V\gamma)_{Q_2^U} &= \left[\frac{G_F}{\sqrt{2}} \lambda_U^{(D)}\right] C_2 \cdot \langle V(p)\gamma(q)|2\tilde{Q}_1^U|\bar{B}(p_B)\rangle \\ &= \left[\frac{G_F}{\sqrt{2}} \lambda_U^{(D)}\right] C_2 \cdot (-ie) e^{*\alpha}(q) \sum_q Q_f \\ &\quad \times \int d^4x e^{iq\cdot x} \langle V(p)|T(\bar{q}\gamma_\alpha q)(x) \\ &\quad \times 2\tilde{Q}_1^U(0)|\bar{B}(p_B)\rangle \end{aligned} \tag{23}$$

$$\equiv \left[\frac{G_F}{\sqrt{2}}\lambda_U^{(D)}\right](-eQ_U)C_2 \cdot \Gamma_{VB}^U, \tag{24}$$

where the minus sign comes from the sign convention for e as discussed in Sec. II. We decompose Γ_{VB}^U into contributions from the photon-helicity amplitudes $S_{L,R}$, Eq. (7), as

$$\Gamma_{VB}^U = l_U(V)P + \tilde{l}_U(V)\tilde{P} \tag{25}$$

with

$$\begin{aligned} P &\equiv \epsilon^{\mu\nu\rho\sigma} e_\mu^* \eta_\nu^* p_\rho q_\sigma = \tfrac{1}{2}(S_L + S_R), \\ \tilde{P} &\equiv i\{(e^*\eta^*)(pq) - (e^*p)(\eta^*q)\} = \tfrac{1}{2}(S_L - S_R). \end{aligned} \tag{26}$$

In addition to Q_2^U, the penguin operators $Q_{3,4,6}$ give a nonzero contribution to soft-gluon emission. Including all these contributions, and comparing (24) with (6) and (7), we obtain the following expression for $a_7^{U,\mathrm{soft}}$:

$$\begin{aligned} a_{7L(R)}^{U,\mathrm{soft}}(V) = \frac{\pi^2}{m_b T_1^{B\to V}(0)}\Big\{ & Q_U C_2 (l_U \pm \tilde{l}_U)(V) \\ & + Q_D C_3 (l_D \pm \tilde{l}_D)(V) \\ & + \sum_q Q_q (C_4 - C_6)(l_q \pm \tilde{l}_q)(V)\Big\}. \end{aligned} \tag{27}$$

Here the sum over q runs over all five active quarks u, d, s, c, b. D denotes the down-type quark in the $b \to D\gamma$ transition. The minus sign in front of C_6 is due to Furry's theorem, according to which only the axial-vector current in the $\bar{U}U$ term in (22) contributes to Γ_{VB}^U. We do not include the contribution from Q_5 because its Fierz transformation changes the chirality of the current so that the resulting loop contribution is proportional to m_D and hence helicity suppressed. In the following we distinguish between heavy (b, c) and light (u, d, s) quark loops. Assuming SU(3)-flavor symmetry, one has $l_u = l_d = l_s$, and ditto for $\tilde{l}_{u,d,s}$, which causes a cancellation of these contributions in the last term in (27). As to be discussed below, in Sec. IV B, we estimate the SU(3)-breaking effects to be around 10%.

We now turn to the calculation of $l_{b,c}$, $\tilde{l}_{b,c}$ and l_u, $\tilde{l}_u$.

A. Heavy-quark loops

The calculation of $l_c(K^*)$ and $\tilde{l}_c(K^*)$ was presented in Ref. [19]; here we briefly recapitulate the method and present results also for l_b, $\tilde{l}_b$ and for ρ, ω, $\bar{K}^*$, ϕ.

It was first noticed in Ref. [54] that soft-gluon emission from a charm loop, Fig. 1(b), is suitable for an OPE in $1/m_c$ since the on-shell photon is far away from the partonic threshold $4m_c^2$. The OPE reads, to leading order in $1/m_c$ [54],

$$ie^\mu \int d^4x e^{iq\cdot x} T\bar{c}\gamma_\mu c(x) 2\tilde{Q}_1^c = Q_F + O(1/m_c^4) \tag{28}$$

where

$$Q_F \equiv c_F \bar{D}\gamma_\rho(1-\gamma_5)\frac{\lambda_a}{2} g\tilde{G}_{\alpha\beta}^a D^\rho (F^{\alpha\beta}) b$$

with

$$c_F = -1/(48\pi^2 m_c^2) \tag{29}$$

and $F_{\alpha\beta} = i(q_\alpha e_\beta^* - q_\beta e_\alpha^*)$ for an outgoing photon. Note that here the sign of g corresponds to the covariant derivative $D_\mu = \partial - igT^a A_\mu^a$ which differs from the sign convention used in Sec. II, but agrees with that used as a standard in hard-perturbative QCD calculations. Our final results for l_c, however, are independent of the sign of g, as the matrix element of Q_F over mesons will be expressed in terms of three-particle light-cone meson DAs containing an explicit factor g which refers to the same convention.

The matrix element of Q_F can be expressed in terms of l_c, $\tilde{l}_c$ as

$$\Gamma_{VB}^c = \langle V(p)|Q_F|B(p_B)\rangle = l_c(V)P + \tilde{l}_c(V)\tilde{P}. \tag{30}$$

The parameters $l_c(K^*)$ and $\tilde{l}_c(K^*)$ were first calculated in Ref. [54] from three-point QCD sum rules. In Ref. [19] we calculated them from LCSRs, which are more suitable for the problem than three-point sum rules; see the discussion in [19]. The sum rules were obtained for the quantities L and $\tilde{L}$, which are related to l_c and $\tilde{l}_c$ by

$$c_F L = \tfrac{1}{2} l_c, \qquad c_F \tilde{L} = \tfrac{1}{2}\tilde{l}_c \tag{31}$$

with c_F given in Eq. (29). The LCSR for L reads [19]

$$\begin{aligned} \frac{m_B^2 f_B}{m_b} L e^{-m_B^2/M^2} = m_b^4 \int_{u_0}^1 du e^{-m_b^2/(uM^2)} \Big[& f_V\left(\frac{m_V}{m_b}\right) R_1(u) \\ & + f_V^\perp \left(\frac{m_V}{m_b}\right)^2 R_2(u)\Big], \end{aligned} \tag{32}$$

where R_1 and R_2 are given in terms of three-particle twist-3 and twist-4 DAs of the vector meson. Explicit expressions are given in [19]. The sum rule for $\tilde{L}$ is analogous.

In this paper we update the values of $l_c(K^*)$ and $\tilde{l}_c(K^*)$ as determined in Ref. [19] and also calculate these parameters for the other vector mesons. The twist-3 and twist-4 parameters entering $R_{1,2}$ are given in Tables V and VI. The results for l_c and $\tilde{l}_c$ are given in Table VII.[2] Those for l_b and $\tilde{l}_b$ are obtained as

$$l_b = \frac{m_c^2}{m_b^2} l_c, \qquad \tilde{l}_b = \frac{m_c^2}{m_b^2}\tilde{l}_c. \tag{33}$$

[2]The values obtained in [54] with local three-point sum rules are $l_c(K^*) = -(1374 \pm 250)$ keV and $\tilde{l}_c(K^*) = -(1749 \pm 250)$ keV. The quoted uncertainty includes solely the variation of the Borel parameter and therefore probably underestimates the uncertainty. The central values are substantially larger than those obtained from LCSRs, Table VII. It is well known that three-point sum rules are inappropriate for b transitions since higher-order condensate contributions grow with m_b and destroy the hierarchy of perturbative and nonperturbative contributions.

TABLE V. Three-particle twist-3 hadronic parameters at the scale $\mu = 1$ GeV. The parameters λ and κ are G odd whereas the parameters ζ and ω are G even. The results for K^* are updates of those published in [19], those for ρ are updates of [33], and those for ϕ are new. We assume the parameters of ρ and ω to be equal. A full derivation of these results will be published elsewhere. Note that the absolute sign of all these parameters depends on the sign convention chosen for the strong coupling g (see text) and that K^* refers to an $(s\bar{q})$ bound state.

	ρ, ω	K^*	ϕ
$\zeta_{3V}^{\parallel}$	0.040(8)	0.026(6)	0.03(1)
$\tilde{\lambda}_{3V}^{\parallel}$	0	0.08(3)	0
$\tilde{\omega}_{3V}^{\parallel}$	−0.085(25)	−0.07(2)	−0.035(2)
$\kappa_{3V}^{\parallel}$	0	0.0005(5)	0
$\omega_{3V}^{\parallel}$	0.20(7)	0.11(3)	0.045(3)
$\lambda_{3V}^{\parallel}$	0	−0.020(8)	0
$\kappa_{3V}^{\parallel}$	0	0.005(2)	0
$\omega_{3V}^{\perp}$	0.65(25)	0.35(10)	0.26(10)
$\lambda_{3V}^{\perp}$	0	−0.05(2)	0

Although the total uncertainties in these parameters are rather large, their contribution to a_{7L}^{U} is of $O(2\%)$ at best and only has a minor impact on the branching ratios. Soft-gluon emission is also irrelevant for isospin asymmetries; its main impact is on the CP asymmetry which is small by itself, so even large uncertainties are acceptable if the aim is to rule out a numerically sizable time-dependent CP asymmetry in the SM. In obtaining these results we use the one-loop pole mass $m_b = (4.7 \pm 0.15)$ GeV, f_B and f_{B_s} as given in Table III, the Borel parameter $M^2 = (12 \pm 3)$ GeV^2, the continuum threshold $s_0 = (35 \pm 2)$ GeV^2, and the renormalization scale $\mu^2 = m_B^2 - m_b^2 \pm 1$ GeV^2 [36]. The uncertainties of the DAs are given in Table V. Within the accuracy of the sum rules for these parameters it is impossible to distinguish between ρ^0 and ω, so we assume them to be equal. In view of the large uncertainties associated with the parameters of the three-particle DAs, we have adopted a conservative way to estimate the total uncertainty of l_c and $\tilde{l}_c$ in Table VII and added the uncertainties linearly. The uncertainties are sizable in m_b, f_B, $\zeta_3^{\parallel}$, and M^2. It is worth noting that the differences $l_c(V) - \tilde{l}_c(V)$ hardly depend on the Borel parameter M^2.

Let us turn to the issue of the convergence of the $1/m_c$ expansion which was discussed, for the inclusive case, in Refs. [56,57]. Higher-order terms in the expansion of (28) contain operators of type $\bar{D}(q \cdot D)^n \tilde{G} b$; the expansion can be resummed with the result given in Ref. [57]. For inclusive decays, the relevant matrix elements are $\langle B|\bar{b}D^n\tilde{G}b|B\rangle$, which can be estimated, on dimensional grounds, as $\langle B|\bar{b}D^n\tilde{G}b|B\rangle \approx \Lambda_{\rm QCD}^n \langle B|\bar{b}\,\tilde{G}\,b|B\rangle$. The expansion parameter is then $t \equiv (m_b\Lambda_{\rm QCD})/(4m_c^2) \approx 0.2$, which is not power suppressed, but not large numerically. For $t = 0.2$ the effect of resummation is to enhance the leading-order matrix element by 15%, whereas for $t = 0.4$ it amounts to a 30% enhancement. We expect the resummation to have a similar effect in exclusive decays. We shall include the effect of truncating the $1/m_c$ expansion by doubling the theoretical uncertainty of our final result for the CP asymmetries, which depend on $l_c - \tilde{l}_c$; the impact of $l_c + \tilde{l}_c$ on the branching ratios is small. We also would like to mention, as noted in [57], that besides the derivative expansion in the gluon field there are further higher-twist contributions from e.g. two gluon fields. These contributions, however, are truly power suppressed and of order $\Lambda_{\rm QCD}^2/m_c^2$, so we feel justified neglecting them.

TABLE VII. Soft-gluon contributions from c-quark loops in keV units. The quantities l_c and $\tilde{l}_c$ are defined in (24) and (25). We assume equal parameters for ρ and ω. l_b is obtained as $l_b = l_c m_c^2/m_b^2$ and correspondingly for $\tilde{l}_b$.

	l_c	$\tilde{l}_c$	$l_c - \tilde{l}_c$	$l_c + \tilde{l}_c$
$B \to K^*$	−355 ± 280	−596 ± 520	242 ± 370	−952 ± 800
$B \to (\rho, \omega)$	−382 ± 300	−502 ± 430	120 ± 390	−884 ± 660
$B_s \to \bar{K}^*$	−347 ± 260	−342 ± 400	−4 ± 300	−689 ± 600
$B_s \to \phi$	−312 ± 240	−618 ± 500	306 ± 320	−930 ± 750

B. Light-quark loops

For light-quark loops the photon is almost at threshold and the local OPE does not apply, unlike the case of heavy quarks discussed in the previous subsection. In this subsection we develop a method for calculating these contributions which starts from the calculation of $\Gamma_{VB}^{u}(q^2)$ from LCSRs for an off-shell photon momentum $q^2 \neq 0$. We then shall use a dispersion relation to relate the off-shell matrix element to $\Gamma_{VB}^{u}(0)$, which in turn can be expressed in terms of the wanted quantities $l_u(V)$ and $\tilde{l}_u(V)$, Eq. (25). The starting point of the method developed here is similar to the one used by Khodjamirian for the calculation of soft-gluon

TABLE VI. Three-particle twist-4 hadronic parameters at the scale $\mu = 1$ GeV. The same remark about the absolute sign and the meaning of K^* applies as for twist-3 parameters.

	ρ, ω, ϕ	K^*	Remarks
$\zeta_{4V}^{\perp}$	0.10 ± 0.05	0.10 ± 0.05	From [44], no SU(3) breaking; to be updated in [45]
$\tilde{\zeta}_{4V}^{\perp}$	$= -\zeta_{4V}^{\perp}$	$= -\zeta_{4V}^{\perp}$	ditto
$\kappa_{4V}^{\perp}$	0	0.012(4)	G odd; quoted from [38]

contributions to $B \to \pi\pi$ [58]. In order to simplify notations, we drop the superscript u on the correlation function.

A suitable correlation function for extracting $\Gamma^u_{VB}(0)$ for the weak interaction operator Q_2 is

$$\begin{aligned}\Gamma_V((q-k)^2, p_B^2, P^2) &= i^2 e^{*\rho} \int d^4x d^4y e^{i(q-k)\cdot x} e^{-ip_B\cdot y} \\ &\times \langle V(p)|T[\bar{u}\gamma_\rho u](x) 2\tilde{Q}_1^u(0) J_B(y)|0\rangle \end{aligned} \quad (34)$$

with $\tilde{Q}_1^u$ defined as in the previous subsection and $p_B \equiv p + q$, $P \equiv p_B - k$. The current $J_B = m_b \bar{b} i\gamma_5 q$ is the interpolating field of the B meson with

$$\langle B(p_B)|J_B|0\rangle = m_B^2 f_B. \quad (35)$$

The leading-order contribution to this correlation function, with a soft gluon, is shown in Fig. 3. Following Ref. [58], we have introduced an unphysical momentum k at the weak vertex. This additional momentum serves to avoid unphysical low-lying cuts in p_B^2, also known as parasitic terms. We will choose the momentum configuration in such a way that k disappears when extracting $\Gamma^u_{VB}(0)$. The kinematics of the correlation function describes a 2-2 scattering process and therefore depends on six independent momentum squares. Three of those, namely,

$$P^2, (q-k)^2, (p_B^2 - m_b^2) \ll -\Lambda^2_{\rm QCD}, \quad (36)$$

are chosen to lie below their respective thresholds, assuring that the correlation function is dominated by lightlike distances and therefore suitable for a light-cone expansion. The other three independent variables are p^2, k^2, and q^2. Neglecting higher-order corrections in the vector-meson mass, we set $p^2 = 0$ and, for simplicity, $k^2 = 0$. We also set $q^2 = (q-k)^2$, which will be necessary for avoiding a subtraction constant in the dispersion relation in q^2 and also leaves only one remnant of the presence of the unphysical momentum k: $P^2 = (p_B - k)^2 \neq p_B^2$. The rationale for this choice of kinematics will become more transparent below.

Inserting a complete set of hadron states, the correlation function becomes

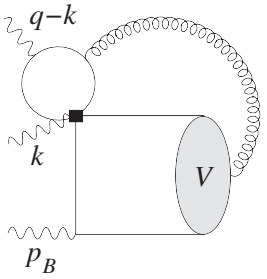

FIG. 3. Leading contribution to the correlation function Γ_V in (34). The black square denotes insertion of the operator Q_i with $i = 1, \ldots, 6$. The B meson momentum is $p_B = p + q$ and the vector meson carries the momentum p.

$$\Gamma_V(q^2, p_B^2, P^2) = (m_B^2 f_B)\frac{\Gamma^*_{VB}(q^2, P^2)}{m_B^2 - p_B^2} + \ldots, \quad (37)$$

where the dots stand for higher states and the star on Γ^*_{VB} is to remind one of the presence of the unphysical momentum k in P^2. We can decompose the correlation function as

$$\Gamma_V = \gamma_V P + \tilde{\gamma}_V \tilde{P} + O(k),$$

with the projectors P and $\tilde{P}$ given in Eq. (26). Additional structures in k are unphysical and can be dropped. Calculating the u-quark loop to twist-3 accuracy, we get

$$\gamma_V = \frac{f_V m_b^2 m_V}{48\pi^2} \int_{(v,\underline{\alpha})} \frac{v(P^2 - (q-k)^2)}{l^2(p_b^2 - m_b^2)} \mathcal{V}(\underline{\alpha}), \quad (38)$$

$$\tilde{\gamma}_V = \frac{f_V m_b^2 m_V}{48\pi^2} \int_{(v,\underline{\alpha})} \frac{v((q-k)^2 - P^2)}{l^2(p_b^2 - m_b^2)} \mathcal{A}(\underline{\alpha}), \quad (39)$$

where $l \equiv q - k + v\alpha_3 p$ and $p_b \equiv q + \bar{\alpha}_1 p$, $\bar{\alpha}_1 \equiv 1 - \alpha_1$ and therefore

$$\begin{aligned} l^2 &= v\alpha_3 P^2 + (1 - v\alpha_3)(q-k)^2, \\ p_b^2 &= \alpha_1 q^2 + \bar{\alpha}_1 p_B^2, \end{aligned} \quad (40)$$

where in our choice of kinematics $(q-k)^2 \to q^2$ in the sequel. $\mathcal{V}$ and $\mathcal{A}$ are twist-3 three-particle DAs of the vector meson; they are discussed in detail in Ref. [33]. The quantities γ_V and $\tilde{\gamma}_V$ also receive contributions of higher twist, which we do not include in this paper. The integration measure is defined as

$$\int_{(v,\underline{\alpha})} = \int_0^1 dv \int_0^1 d\alpha_1 d\alpha_2 d\alpha_3 \delta(1 - \alpha_1 - \alpha_2 - \alpha_3). \quad (41)$$

Equations (38)–(40) clearly show that the introduction of the unphysical momentum k avoids a low-lying cut (parasite) from the u-quark loop in the variable p_B^2.

The parasitic term in q^2, however, which originates from the b-quark propagator going on shell, is not absent for our choice $q^2 = (q-k)^2$. It induces a parasitic term to be added to (37) which is of the form

$$\begin{aligned}\langle V(p)|J_B|B_D(q)\rangle \frac{e^{*\rho}}{m_{B_D}^2 - q^2} \int d^4x e^{i(q-k)\cdot x} \langle B_D(q)|T 2\tilde{O}_1(0) \\ \times [\bar{u}\gamma_\rho u](x)|0\rangle + O(k). \end{aligned} \quad (42)$$

The matrix element on the left-hand side is just the form factor $A_0(p_B^2)$ for $B \to V$ transitions, which was calculated from LCSRs in [36] and exhibits a pole $\sim 1/(m_B^2 - p_B^2)$ in p_B^2 inducing a parasitic contribution to the first term in Eq. (37). Before we can proceed any further, we need to determine the size of this parasitic contribution. If we were dealing with a c-quark loop, we could apply a local OPE to the integral and calculate its value from (28) and the following estimate based on dimensional analysis:

$$\langle B_D|\bar{D}\gamma_\rho(1-\gamma_5)\tilde{G}_{\alpha\beta}b|0\rangle \simeq f_B(p_B)_\rho t_{\alpha\beta}\cdot\Lambda^2_{\rm QCD}, \quad (43)$$

where t_{α_β} is an antisymmetric dimensionless tensor. The ratio of the parasitic term (42) to the main term in (37) is then of order $\Lambda^2_{\rm QCD}/m_b^2 \sim 1\%$ and negligibly small. For the u loop, on the other hand, the local OPE is not applicable and one is back to our initial problem of devising a method to calculate a nonlocal correlation function, although in this case a simpler one than that in Eq. (23). Given, however, the smallness of the parasitic term for heavy quarks $\sim$1%, it is unlikely that this term is an order of magnitude larger for light quarks, especially in view of the numerical closeness of the light-quark and heavy-quark loops. For our cases of interest, even a contamination at the level of 50% would not constitute a major problem, as these contributions to $B\to V\gamma$ are only relevant for the time-dependent CP asymmetry which is expected to be near zero in the SM. Our major aim is to confirm that this is indeed the case and to exclude large contributions from soft-gluon emission, but not to give a precise determination of their size. In view of this, even a large parasitic contamination is perfectly acceptable.

The next step is to write (38) and (39) in terms of a dispersion relation in p_B^2,

$$\gamma_V(q^2,p_B^2,P^2)=\frac{1}{\pi}\int_{m_b^2}^\infty\frac{ds}{s-p_B^2}\,{\rm Im}_s\gamma_V(q^2,s,P^2), \quad (44)$$

in order to match them to the hadronic representation (37). The quantity $l_u^*(q^2,P^2)$ can then be obtained by applying the standard QCD sum rule techniques, namely, Borel transformation and continuum subtraction, which yield

$$l_u^*(q^2,P^2)=\frac{1}{m_B^2 f_B}\frac{1}{\pi}\int_{m_b^2}^{s_0^B}ds e^{(m_B^2-s)/M^2}\,{\rm Im}_s\gamma_V(q^2,s,P^2), \quad (45)$$

where the star again indicates the presence of the unphysical momentum k in $P^2=(p_B-k)^2$; also note that the photon is still off shell. Once ${\rm Im}_s\gamma_V(q^2,s,P^2)$ is known, $l_u^*(q^2,P^2)$ can be analytically continued in $P^2\to m_B^2+i0$. For the B-meson ground state, this removes the last trace of the unphysical momentum k. The analytic continuation in P^2 is justified because it is far above the other hadronic scales in the corresponding channel. This yields the physical u-quark amplitude, yet still for an off-shell photon.

After the conceptual outline given above, we will now outline how to proceed from the intermediate results (38) and (39). In order to obtain the imaginary parts of γ_V and $\tilde{\gamma}_V$, it proves convenient to perform some of the integrations over the variables v and α_i until logarithms appear whose imaginary parts (cuts) can easily be identified. It turns out that the integrals over dv and $d\alpha_1$ with $\alpha_2=1-\alpha_1-\alpha_3$ are elementary since the involved variables are spacelike which guarantees the absence of singularities. We obtain an expression of the form

$$\begin{aligned}\gamma_V\sim\int_0^1 d\alpha_3\frac{1}{(P^2-q^2)(p_B^2-q^2)^3}\{((\ln[m_b^2-p_B^2]\\ -\ln[m_b^2-\alpha_3 p_B^2-\bar{\alpha}_3 q^2])P_1+P_2)(\ln[-q^2]\\ -\ln[-\alpha_3 P^2-\bar{\alpha}_3 q^2]P_3+P_4)\}P_5, \end{aligned}\quad (46)$$

where P_i stands for polynomials. The poles in q^2 are integrable, i.e. removable. The dispersion representation in p_B^2 is now obtained from the cuts of the logarithms. We find

$$\begin{aligned}-\int_{m_b^2}^\infty\frac{ds}{s-p_B^2}\int_0^{(m_b^2-q^2)/(s-q^2)}d\alpha_3((\ln[-q^2]\\ -\ln[-\alpha_3 P^2-\bar{\alpha}_3 q^2])P_3+P_4)\\ \times\frac{P_1P_5}{(P^2-q^2)(p_B^2-q^2)^3}.\end{aligned}$$

The integral over $d\alpha_3$ is elementary and we finally obtain the imaginary part for the dispersion relation (44):

$$\begin{aligned}\frac{1}{\pi}\,{\rm Im}_s\gamma_V(q^2,s,P^2)\Big|_{s\geq m_b^2}=\frac{f_V m_b^2 m_V}{8\pi^2(P^2-q^2)^3(s-q^2)^5}\\ \times(\ln[-q^2]+\ln[s-q^2]\\ -\ln[-m_b^2P^2-q^2(s-m_b^2\\ -P^2)]+P_6)P_7.\end{aligned}\quad (47)$$

This is the expression to be used in Eq. (45). As discussed above, the momentum k completely disappears upon analytic continuation of $P^2\to m_B^2+i0$ and we obtain the amplitude for an off-shell photon. The analytic continuation is rather straightforward: l_u^* acquires an imaginary part from those logarithms whose arguments depend on P^2. The imaginary part is proportional to the mass of the u quark and originates from the quark going on shell. After the analytic continuation of (47), all remnants of the unphysical momentum k have disappeared and we can drop the star from now on:

$$\begin{aligned}l_u(q^2)\equiv l_u(q^2,m_B^2+i0)\\ =\frac{1}{m_B^2 f_B}\frac{1}{\pi}\int_{m_b^2}^{s_0^B}ds e^{(m_B^2-s)/M^2}\\ \times{\rm Im}_s\gamma_V(q^2,s,m_B^2+i0),\end{aligned}\quad (48)$$

for $q^2\ll-\Lambda^2_{\rm QCD}$. It is interesting to note that, if one does not project onto the B ground state, the analytic continuation leads to unphysical cuts in negative q^2 which come from the fact that for higher states the unphysical momentum k is still present.

There remains only one step to be done, namely, to put the photon on shell, i.e. $q^2\to 0$. To do so, we follow the method used in Ref. [59], where the pion-photon-photon transition form factor $F_{\gamma^*\gamma\pi}$ was estimated with one on-shell photon. Since $l_u(q^2)$ is an analytic function in q^2, it has the standard dispersion representation

$$l_u(q^2) = \frac{1}{\pi}\int_{\text{cut}}^{\infty} dt \frac{\text{Im}_t l_u(t)}{t-q^2} \tag{49}$$

for q^2 below the cut. Potential subtraction terms spoiling the above representation are absent. This can be seen as follows: for very large Euclidian values $-q^2 \gg \Lambda^2_{\text{QCD}}$, one can perform a local OPE very much the same way as for c-quark loops with the expansion coefficient $1/m_c^2 \to 1/q^2$. Using this result we have explicitly verified that $l_u(q^2)$, $\tilde{l}_u(q^2) \sim^{q^2\to\infty} 1/q^2$. Another indication, although not sufficient, is that the explicit calculation of $l_u^*(q^2, P^2)$ does not contain a constant or polynomial terms in q^2. The imaginary part in q^2 comes from the logarithms in (47) and the poles in $1/(q^2 - s)$. The poles in $P^2 = m_B^2 + i0$ are again integrable or removable.

The perturbative or parton representation has a cut starting at 0, Eq. (49), and it is therefore impossible to set $q^2 = 0$ because it is right below the perturbative threshold. The idea is then to cut out this lower part by inserting resonances that couple to the $\bar{u}\gamma_\mu u$ current; $q^2 = 0$ is then sufficiently below the resonances and the corresponding continuum threshold. We shall content ourselves with the two lowest resonances, ρ and ω. Treating them as equal, we have

$$l_u(q^2) = \frac{2r_\rho}{m_\rho^2 - q^2} + \frac{1}{\pi}\int_{s_0^\rho}^{\infty} \frac{\text{Im}_t l_u(t)}{t-q^2} \tag{50}$$

where

$$r_\rho P + \tilde{r}_\rho \tilde{P} = e_\mu^* \sum_{\text{pol}} \langle 0|\bar{u}\gamma^\mu u|\rho\rangle\langle\rho V|2\tilde{Q}_1|B\rangle,$$

and the sum runs over the polarization of the ρ. It remains to determine r_ρ (and $\tilde{r}_\rho$), so that Eq. (50) can be used to extract $l_u(0)$. This can be achieved by applying a Borel transformation in the variable q^2 which yields the estimate

$$2r_\rho = \frac{1}{\pi}\int_0^{s_0^\rho} dt\, \text{Im} l_u(t) e^{(m_\rho^2 - t)/M^2} \tag{51}$$

and finally

$$l_u \equiv l_u(0) = \frac{1}{\pi}\int_0^{s_0^\rho} \frac{dt}{m_\rho^2} e^{(m_\rho^2 - t)/M^2}\, \text{Im} l_u(t) + \frac{1}{\pi}\int_{s_0^\rho}^{\infty} \frac{dt}{t}\, \text{Im} l_u(t). \tag{52}$$

The crucial point here is that for t below the continuum threshold the factor $1/t$ gets replaced by $e^{(m_\rho^2 - t)/M^2}/m_\rho^2$.

At this point we would also like to clarify in what respect our method to calculate soft-gluon emission in $B \to V\gamma$ differs from that developed in Ref. [58] for analogous contributions to the nonleptonic $B \to \pi\pi$ decay. In both cases the problem is a light-quark loop which is almost on shell, the corresponding nonperturbative effects are estimated from light-cone sum rules, and, in order to avoid parasitic terms in the correlation function, an auxiliary momentum is introduced into the weak vertex. The distinction is that, in contrast to the pion, the photon is a perturbative state and therefore cannot be represented by an interpolating current, but appears directly in the diagram with on-shell momenta. In order to set the photon on its mass shell, we use a dispersion representation, Eq. (49), and estimate the truly nonperturbative part of the spectral function from the corresponding sum rule, Eq. (51). Moreover we have checked, by inspecting the OPE in the deep Euclidian, that the dispersion representation has no subtraction terms, which is implicitly assumed in (49). In order to assure the absence of these terms we had to set the two, in principle, independent momentum squares q^2 and $(q-k)^2$ equal to each other. This reintroduced a parasitic contribution of the form (42) which we estimated to be of $O(1\%)$ as compared to the main contribution.

The sum rule (52) gives the numerical results collected in Table VIII. We use the Borel parameter $M^2 = (1.2 \pm 0.3)\ \text{GeV}^2$ and the threshold $s_0^\rho = (1.6 \pm 0.1)\ \text{GeV}^2$. Comparing these results with those from the c loop, Table VII, we see that they are roughly of the same size, but come with opposite sign. The smallness of $(l_u - \tilde{l}_u)(\rho)$ is due to an accidental numerical cancellation. The uncertainties are large, which is no cause for concern, however, because we are only interested in the approximate size of these contributions which set the size of the time-dependent CP asymmetry in $B \to V\gamma$.

TABLE VIII. Soft-gluon contributions from u-quark loops in keV units. The quantities l_u and $\tilde{l}_u$ are defined in (24) and (25). We assume $l_u(\rho) = l_u(\omega)$ and similarly for $\tilde{l}_u$. The uncertainty for $l_u - \tilde{l}_u$ is given in absolute numbers because of cancellations. In the SU(3)-flavor limit assumed in this calculation, one has $l_u = l_d = l_s \equiv l_q$.

	l_u	$\tilde{l}_u$	$l_u - \tilde{l}_u$	$l_u + \tilde{l}_u$
$B \to K^*$	$536 \pm 70\%$	$635 \pm 70\%$	-99 ± 300	$1172 \pm 70\%$
$B \to (\rho, \omega)$	$827 \pm 70\%$	$828 \pm 70\%$	-1 ± 300	$1655 \pm 70\%$
$B_s \to \bar{K}^*$	$454 \pm 70\%$	$572 \pm 70\%$	-118 ± 300	$1025 \pm 70\%$
$B_s \to \phi$	$156 \pm 70\%$	$737 \pm 70\%$	-581 ± 300	$893 \pm 70\%$

In the above, we have assumed SU(3)-flavor symmetry which implies $l_u = l_d = l_s \equiv l_q$. We can estimate the size of SU(3)-breaking effects by taking into account that l_s couples to the $\bar{s}\gamma_\mu s$ current via the ϕ and higher resonances in (50) and requires a slightly higher continuum threshold s_0^ϕ. This leads to a numerical difference with respect to l_u which is around 5%. The effect of neglecting the quark masses is of order m_q/m_b and therefore even smaller. We conclude that it seems unlikely that l_s differs from $l_{u,d}$ by more than 10%.

V. PHENOMENOLOGICAL RESULTS

In this section we combine the different contributions to the factorization coefficients $a^U_{7L(R)}$ calculated in Secs. II, III, and IV and give results for the observables in $B \to V\gamma$ transitions, namely, the branching ratio, the isospin asymmetry, and the time-dependent CP asymmetry.

A. Branching ratios

The (non-CP-averaged) branching ratio of the $b \to D\gamma$ decay $\bar{B} \to V\gamma$ is given by

$$\mathcal{B}(\bar{B} \to V\gamma) = \frac{\tau_B}{c_V^2}\frac{G_F^2 \alpha m_B^3 m_b^2}{32\pi^4}\left(1 - \frac{m_V^2}{m_B^2}\right)^3 [T_1^{B\to V}(0)]^2 \times \left\{ \left| \sum_U \lambda_U^{(D)} a^U_{7L}(V) \right|^2 + \left| \sum_U \lambda_U^{(D)} a^U_{7R}(V) \right|^2 \right\} \tag{53}$$

with the isospin factors $c_{\rho^\pm,K^*,\phi} = 1$ and $c_{\rho^0,\omega} = \sqrt{2}$. The branching ratio for the CP-conjugated channel $B \to \bar{V}\gamma$ ($\bar{b} \to \bar{D}\gamma$ at parton level) is obtained by replacing $\lambda_U^{(D)} \to (\lambda_U^{(D)})^*$. Experimental results for $B \to K^*\gamma$ and $B \to (\rho, \omega)\gamma$ are collected in Table I. For $B_s \to \phi\gamma$ there is only an upper bound $\mathcal{B}(B_s \to \phi\gamma) < 120 \times 10^{-6}$ [28]. No experimental information is available for $B_s \to \bar{K}^*\gamma$.

With the input parameters from Table III and the lifetimes given in Table IX, we find the following CP-averaged branching ratios for $B \to K^*\gamma$, making explicit various sources of uncertainty:

$$\begin{aligned}
\bar{\mathcal{B}}(B^- \to K^{*-}\gamma) &= (53.3 \pm 13.5(T_1) \pm 4.8(\mu) \pm 1.8(V_{cb}) \\
&\quad \pm 1.9(l_{u,c}) \pm 1.3(\text{other})) \times 10^{-6} \\
&= (53.3 \pm 13.5(T_1) \pm 5.8) \times 10^{-6}, \\
\bar{\mathcal{B}}(\bar{B}^0 \to K^{*0}\gamma) &= (54.2 \pm 13.2(T_1) \pm 6.0(\mu) \pm 1.8(V_{cb}) \\
&\quad \pm 1.8(l_{u,c}) \pm 1.4(\text{other})) \times 10^{-6} \\
&= (54.2 \pm 13.2(T_1) \pm 6.7) \times 10^{-6}.
\end{aligned} \tag{54}$$

TABLE IX. B lifetimes from HFAG [6].

τ_{B^0}	$\tau_{B^\pm}/\tau_{B^0}$	$\tau_{B_s^0}/\tau_{B^0}$
1.530(9) ps	1.071(9)	0.958(39)

We have added all individual uncertainties in quadrature, except for that induced by the form factor. The uncertainty in μ is that induced by the renormalization-scale dependence, with $\mu = m_b(m_b) \pm 1$ GeV. The uncertainty in $l_{u,c}$ refers to the soft-gluon terms calculated in Sec. IV. "Other" sources of uncertainty include the dependence on the parameters in Table III, on the size of LD WA contributions and the replacement of NLO by LO Wilson coefficients. The above results agree, within errors, with the experimental ones given in Table I, within the large theoretical uncertainty induced by the form factor.

As the uncertainties of all form factors in Table III are of roughly the same size, one might conclude that the predictions for all branching ratios will carry uncertainties similar to those in (54). This is, however, not the case: the accuracy of the theoretical predictions can be improved by making use of the fact that the *ratio* of form factors is known much better than the individual form factors themselves. The reason is that the values given in Table III, which were calculated using the same method, LCSRs, and with a common set of input parameters, include common systematic uncertainties (dependence on f_B, m_b, etc.) which partially cancel in the ratio. In Ref. [22] we have investigated in detail the ratio of the K^* and ρ form factors and found

$$\xi_\rho \equiv \frac{T_1^{B\to K^*}(0)}{T_1^{B\to\rho}(0)} = 1.17 \pm 0.09. \tag{55}$$

The uncertainty is by a factor 2 smaller than if we had calculated ξ_ρ from the entries in Table III; an analogous calculation for ω yields

$$\xi_\omega \equiv \frac{T_1^{B\to K^*}(0)}{T_1^{B\to\omega}(0)} = 1.30 \pm 0.10. \tag{56}$$

The difference between ξ_ρ and ξ_ω is mainly due to the difference between $f_\omega^\perp$ and $f_\rho^\perp$; see Table III. For the B_s form factors, we also need the ratio of decay constants f_{B_s}/f_{B_d}. The status of f_B from lattice was reviewed in Ref. [41]; the present state-of-the-art calculations are unquenched with $N_f = 2 + 1$ active flavors [60], whose average is $f_{B_s}/f_{B_d} = 1.23 \pm 0.07$. Again, this ratio is fully consistent with that quoted in Table III, but has a smaller uncertainty. We then find the following ratios for B_s form factors:

$$\begin{aligned}
\xi_\phi &\equiv \frac{T_1^{B\to K^*}(0)}{T_1^{B_s\to\phi}(0)} = 1.01 \pm 0.13, \\
\xi_{\bar{K}^*} &\equiv \frac{T_1^{B\to K^*}(0)}{T_1^{B_s\to\bar{K}^*}(0)} = 1.09 \pm 0.09.
\end{aligned} \tag{57}$$

The uncertainty of $\xi_{\bar{K}^*}$ is smaller than that of ξ_ϕ because the input parameters for K^* and $\bar{K}^*$ are the same (except for G-odd parameters like $a_1^\perp$) and cancel in the ratio; the uncertainty is dominated by that of f_{B_s}/f_{B_d}.

To benefit from this reduced theoretical uncertainty in predicting branching ratios, one has to calculate ratios of branching ratios, which mainly depend on ξ_V and only mildly on T_1 itself: in addition to the overall normalization, T_1 also enters hard-spectator interactions and power-suppressed corrections, whose size is set by hadronic quantities $\propto 1/T_1$. As these corrections are subleading (in α_s or $1/m_b$), however, a small shift in T_1 has only very minor impact on the branching ratios. The absolute scale for the branching ratios is set by the CP- and isospin-averaged branching ratio with the smallest experimental uncertainty, i.e. $B \to K^*\gamma$; from Table I, one finds

$$\bar{\mathcal{B}}(B \to K^*\gamma) = \frac{1}{2}\left\{\bar{\mathcal{B}}(B^\pm \to K^{*\pm}\gamma) + \frac{\tau_{B^\pm}}{\tau_{B^0}}\bar{\mathcal{B}}(\bar{B}^0 \to K^{*0}\gamma)\right\} = (41.6 \pm 1.7) \times 10^{-6}. \quad (58)$$

That is, we obtain a theoretical prediction for $\bar{\mathcal{B}}(B \to V\gamma)$ as

$$\bar{\mathcal{B}}(B \to V\gamma)|_{\rm th} = \left[\frac{\bar{\mathcal{B}}(B \to V\gamma)}{\bar{\mathcal{B}}(B \to K^*\gamma)}\right]_{\rm th} \bar{\mathcal{B}}(B \to K^*\gamma)|_{\rm exp}, \quad (59)$$

where $[\ldots]_{\rm th}$ depends mainly on ξ_V and only in subleading terms on the individual form factors $T_1^{B\to K^*}$ and $T_1^{B\to V}$. It is obvious that, except for these subleading terms, this procedure is equivalent to extracting an *effective form factor* $T_1^{B\to K^*}(0)|_{\rm eff}$ from $B \to K^*\gamma$ and using $T_1^{B\to V}(0)|_{\rm eff} = T_1^{B\to K^*}(0)|_{\rm eff}/\xi_V$ for calculating the branching ratios for $B \to V\gamma$. From (58) we find

$$T_1^{B\to K^*}(0)|_{\rm eff} = 0.267 \pm 0.017({\rm th}) \pm 0.006({\rm exp}) = 0.267 \pm 0.018, \quad (60)$$

where the theoretical uncertainty follows from the second uncertainty given in (54). Equations (55)–(57) then yield

$$\begin{aligned} T_1^{B\to\rho}(0)|_{\rm eff} &= 0.228 \pm 0.023, \\ T_1^{B\to\omega}(0)|_{\rm eff} &= 0.205 \pm 0.021, \\ T_1^{B_s\to\bar{K}^*}(0)|_{\rm eff} &= 0.245 \pm 0.024, \\ T_1^{B_s\to\phi}(0)|_{\rm eff} &= 0.260 \pm 0.036. \end{aligned} \quad (61)$$

Note that all effective form factors agree, within errors, with the results from LCSRs given in Table III, which confirms the results obtained from this method; the crucial point, however, is that the uncertainties are reduced by a factor of 2 (except for $T_1^{B_s\to\phi}$). We would like to stress that the motivation for this procedure is to achieve a reduction of the theoretical uncertainty of the predicted branching fractions in $B \to (\rho, \omega)\gamma$ and B_s decays. The effective form factors do *not* constitute a new and independent theoretical determination, but are derived from the experimental results for $B \to K^*\gamma$ under the following assumptions:

(i) there is no NP in $B \to K^*\gamma$[3];
(ii) QCDF is valid with no systematic uncertainties;
(iii) LCSRs can reliably predict the ratio of form factors at zero momentum transfer.

From (53) and (61), we then predict the following CP-averaged branching ratios:

$$\begin{aligned} \bar{\mathcal{B}}(B^- \to \rho^-\gamma) &= (1.16 \pm 0.22(T_1) \pm 0.13) \times 10^{-6}, \\ \bar{\mathcal{B}}(B^0 \to \rho^0\gamma) &= (0.55 \pm 0.11(T_1) \pm 0.07) \times 10^{-6}, \\ \bar{\mathcal{B}}(B^0 \to \omega\gamma) &= (0.44 \pm 0.09(T_1) \pm 0.05) \times 10^{-6}, \\ \bar{\mathcal{B}}(B_s \to \bar{K}^*\gamma) &= (1.26 \pm 0.25(T_1) \pm 0.18) \times 10^{-6}, \\ \bar{\mathcal{B}}(B_s \to \phi\gamma) &= (39.4 \pm 10.7(T_1) \pm 5.3) \times 10^{-6}, \end{aligned} \quad (62)$$

where the first uncertainty is induced by the effective form factors and the second includes the variation of all inputs from Table III except for the angle γ of the UT, which is fixed at $\gamma = 53°$. The total uncertainty in each channel is $\sim$20%, except for $B_s \to \phi\gamma$, where it is 30%. The results for ρ and ω agree very well with those of *BABAR*, Table I, but less so with the Belle results, although present experimental and theoretical uncertainties preclude a firm conclusion. Our prediction for $B_s \to \phi\gamma$ is well below the current experimental bound 120×10^{-6} [28]. A branching ratio of the size given in (62) implies that $O(10^3)$ $B_s \to \phi\gamma$ events will be seen within the first few years of the LHC. In Table X we detail the contributions of individual terms to the branching ratios. In all cases $\mathcal{B}$ is dominated by the QCDF contribution, with WA most relevant for $B^- \to \rho^-\gamma$. This is expected as WA enters with the large Wilson coefficient $C_2 \sim 1$. The effect is extenuated by long-distance (LD) photon emission, which itself is compensated by soft-gluon emission. The other channels follow a similar pattern, although the size of the effects is smaller.

Let us now turn to the determination of CKM parameters from the branching ratios. In this context, two particularly interesting observables are

$$R_{\rho/\omega} \equiv \frac{\bar{\mathcal{B}}(B \to (\rho, \omega)\gamma)}{\bar{\mathcal{B}}(B \to K^*\gamma)}, \qquad R_\rho \equiv \frac{\bar{\mathcal{B}}(B \to \rho\gamma)}{\bar{\mathcal{B}}(B \to K^*\gamma)}, \quad (63)$$

given in terms of the CP- and isospin-averaged branching ratios of $B \to (\rho, \omega)\gamma$ and $B \to \rho\gamma$, respectively, and $B \to K^*\gamma$ decays; see Table I. $R_{\rho/\omega}$ has been measured by both *BABAR* and Belle [4,5]; a first value of R_ρ has been given by *BABAR* [4]. The experimental determinations actually assume exact isospin symmetry, i.e. $\bar{\Gamma}(B^\pm \to \rho^\pm\gamma) \equiv 2\bar{\Gamma}(B^0 \to \rho^0\gamma)$, and also $\bar{\Gamma}(B^0 \to \rho^0\gamma) \equiv \bar{\Gamma}(B^0 \to \omega\gamma)$; as we shall discuss in the next subsection, these relations are not exact, and the symmetry-breaking corrections can

[3]Which is motivated by the results from inclusive $B \to X_s\gamma$ decays [2].

TABLE X. Individual contributions to *CP*-averaged branching ratios, using effective form factors and central values of all other input parameters given in Table III (in particular, $\gamma = 53°$). LD stands for the long-distance photon-emission contribution to WA. Each column labeled "+X" includes the contributions listed in the previous column plus the contribution induced by X. The entries in the last column are our total central values.

	QCDF	+WA (no LD)	+WA (incl. LD)	+ soft gluons
$B^- \to \rho^- \gamma$	1.05	1.17	1.11	1.16
$B^0 \to \rho^0 \gamma$	0.49	0.53	0.53	0.55
$B^0 \to \omega \gamma$	0.40	0.42	0.42	0.44
$B^- \to K^{*-} \gamma$	39.7	38.4	38.3	39.4
$B^0 \to K^{*0} \gamma$	37.1	39.7	39.9	41.0
$B_s^0 \to \bar{K}^{*0} \gamma$	1.12	1.22	1.23	1.26
$B_s^0 \to \phi \gamma$	34.6	38.2	38.3	39.4

be calculated. Hence, the present experimental results for $R_{\rho/\omega}$ are theory-contaminated. As the isospin asymmetry between the charged and neutral ρ decay rates turns out to be smaller than the asymmetry between ρ^0 and ω, it would actually be preferable, from an experimental point of view, to drop the ω channel and measure R_ρ instead of $R_{\rho/\omega}$, as done in the most recent *BABAR* analysis on that topic [4]. We will give numerical results and theory uncertainties for both $R_{\rho/\omega}$ and R_ρ.

One parametrization of $R_{\rho/\omega}$ often quoted, in particular, in experimental papers, is

$$R_{\rho/\omega} = \left|\frac{V_{td}}{V_{ts}}\right|^2 \left(\frac{1 - m_\rho^2/m_B^2}{1 - m_{K^*}^2/m_B^2}\right)^3 \frac{1}{\xi_\rho^2}[1 + \Delta R], \qquad (64)$$

with $\Delta R = 0.1 \pm 0.1$ [9] and again assuming isospin symmetry for ρ and ω. This parametrization creates the impression that ΔR is a quantity completely unrelated to and with a fixed value independent of $|V_{td}/V_{ts}|$. We would like to point out here that this impression is *wrong*: ΔR contains both QCD (factorizable and nonfactorizable) effects and such from weak interactions. In Ref. [22], we have expressed ΔR in terms of the factorization coefficients a_{7L}^U, assuming isospin symmetry for ρ^0 and ω, as

$$1 + \Delta R = \left|\frac{a_{7L}^c(\rho)}{a_{7L}^c(K^*)}\right|^2 \Bigg(1 + \mathrm{Re}(\delta a_\pm + \delta a_0) \times \left[\frac{R_b^2 - R_b \cos\gamma}{1 - 2R_b \cos\gamma + R_b^2}\right] + \frac{1}{2}(|\delta a_\pm|^2 + |\delta a_0|^2)\left\{\frac{R_b^2}{1 - 2R_b \cos\gamma + R_b^2}\right\}\Bigg) \qquad (65)$$

with $\delta a_{0,\pm} = a_{7L}^u(\rho^{0,\pm})/a_{7L}^c(\rho^{0,\pm}) - 1$. Here γ is one of the angles of the UT ($\gamma = \arg V_{ub}^*$ in the standard Wolfenstein parametrization of the CKM matrix) and R_b one of its sides:

$$R_b = \left(1 - \frac{\lambda^2}{2}\right)\frac{1}{\lambda}\left|\frac{V_{ub}}{V_{cb}}\right|.$$

Equation (65) shows explicitly that ΔR depends both on QCD ($\delta a_{\pm,0}$) and CKM parameters (R_b, γ). The point we would like to make is that the calculation of ΔR requires input values for R_b and γ. Once these parameters (and the Wolfenstein parameter λ) are fixed, however, $|V_{td}/V_{ts}|$ is also fixed and given by

$$\left|\frac{V_{td}}{V_{ts}}\right| = \lambda\sqrt{1 - 2R_b\cos\gamma + R_b^2}\left[1 + \frac{1}{2}(1 - 2R_b\cos\gamma)\lambda^2 + O(\lambda^4)\right]. \qquad (66)$$

Hence, as $|V_{td}/V_{ts}|$ and (R_b, γ) are not independent of each other, it is *impossible* to extract $|V_{td}/V_{ts}|$ from (64) with a fixed value of ΔR. We hasten to add that our arguments rely on the unitarity of the CKM matrix, and its well-known consequence, the existence of the UT. The unitarity of the CKM matrix is, however, already hard wired into the effective Hamiltonian (2); without it, the theory would look quite different because of the absence of the GIM mechanism, as mentioned in Sec. II, Eq. (3). Stated differently, as long as Eq. (2) is adopted as the relevant effective Hamiltonian for $b \to D\gamma$ transitions, unitarity of the CKM matrix is implied. Obviously, the unitarity of the CKM matrix is subject to experimental scrutiny, but any test of it has to involve the comparison of *different* measurements described within the same framework (by the same effective Hamiltonian), while a mixture of different frameworks (unitary vs nonunitary CKM matrix) within *one* observable, like $R_{\rho/\omega}$, does not make any sense.

Of course $R_{\rho/\omega}$ and R_ρ of (63) *can* be used in a meaningful way to extract information about CKM parameters, but in order to do so one has to settle for a set of truly independent parameters. Based on (66), one can exchange, say, γ for $|V_{td}/V_{ts}|$.[4] So we can either consider R_V as a function of the CKM parameters R_b and γ (let us call this

[4]Strictly speaking, (66) only fixes $\cos\gamma$ as a function of $|V_{td}/V_{ts}|$, leaving a twofold degeneracy of γ. Equation (65), however, only depends on $\cos\gamma$, so that indeed one can unambiguously replace γ by $|V_{td}/V_{ts}|$.

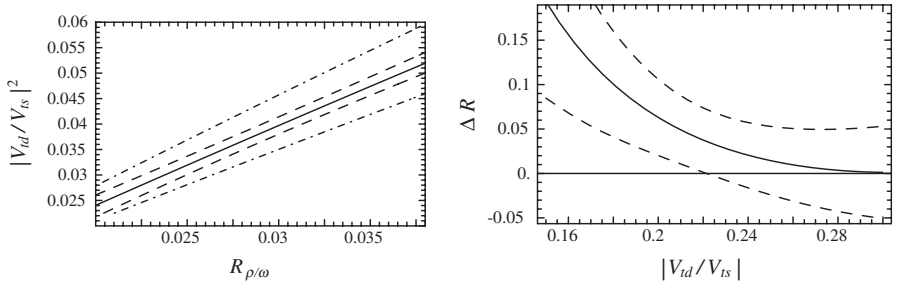

FIG. 4. Left panel: $|V_{td}/V_{ts}|^2$ as a function of $R_{\rho/\omega}$, Eq. (63), in the $|V_{tx}|$ basis (see text). Solid line: central values. Dash-dotted lines: theoretical uncertainty induced by $\xi_\rho = 1.17 \pm 0.09$, (55). Dashed lines: other theoretical uncertainties, including those induced by $|V_{ub}|$, $|V_{cb}|$ and the hadronic parameters of Table III. Right panel: ΔR from Eq. (65) as a function of $|V_{td}/V_{ts}|$ for the $|V_{tx}|$ set of CKM parameters. Solid line: central values. Dashed lines: theoretical uncertainty.

the γ set of parameters) or as a function of R_b and $|V_{td}/V_{ts}|$ (to be called the $|V_{tx}|$ set). Using the γ set, a measurement of $R_V(\gamma, R_b)$ allows a determination of γ, whereas $R_V(|V_{td}/V_{ts}|, R_b)$ allows the determination of $|V_{td}/V_{ts}|$. In either case, the simple quadratic relation (64) between R_V and $|V_{td}/V_{ts}|$ becomes more complicated. In Figs. 4 and 5 we plot the resulting values of $|V_{td}/V_{ts}|^2$ and γ, respectively, as a function of R_V. Although the curve in Fig. 4(a) looks like a straight line, as naively expected from (64), this is not exactly the case, because of the dependence of ΔR on $|V_{td}/V_{ts}|$. In Fig. 4(b) we plot ΔR for the $|V_{tx}|$ set of parameters. The dependence of ΔR on $|V_{td}/V_{ts}|$ is rather strong. Apparently, indeed $\Delta R = 0.1 \pm 0.1$ in the expected range $0.16 < |V_{td}/V_{ts}| < 0.24$, but this estimate does not reflect the true theoretical uncertainty which is indicated by the dashed lines in the figure.

It is now basically a matter of choice whether to use $R_{\rho/\omega}$ to determine $|V_{td}/V_{ts}|$ or γ. Once one of these parameters is known, the other one follows from Eq. (66). In Fig. 5 we plot γ as a function of $R_{\rho/\omega}$, together with the theoretical uncertainties. In Fig. 6 we also compare the central values of $R_{\rho/\omega}$ with those of R_ρ, as a function of $|V_{td}/V_{ts}|$. Although the difference is small, R_ρ is expected to be larger than $R_{\rho/\omega}$. In order to facilitate the extraction of $|V_{td}/V_{ts}|$ (or γ) from measurements of $R_{\rho/\omega}$ or R_ρ, Tables XI and XII contain explicit values for the theoretical uncertainties for representative values of $R_{\rho/\omega}$ and R_ρ. The uncertainty induced by ξ_ρ is dominant. As discussed in Ref. [22], a reduction of this uncertainty would require a reduction of the uncertainty of the transverse decay constants $f_V^\perp$ of ρ and K^*. With the most recent results from *BABAR*, $R_{\rho/\omega} = 0.030 \pm 0.006$ [4], and from Belle, $R_{\rho/\omega} = 0.032 \pm 0.008$ [5], we then find

$$\begin{aligned} \textit{BABAR}: \left|\frac{V_{td}}{V_{ts}}\right| &= 0.199^{+0.022}_{-0.025}(\text{exp}) \pm 0.014(\text{th}) \leftrightarrow \gamma \\ &= (61.0^{+13.5}_{-16.0}(\text{exp})^{+8.9}_{-9.3}(\text{th}))^\circ, \\ \text{Belle}: \left|\frac{V_{td}}{V_{ts}}\right| &= 0.207^{+0.028}_{-0.033}(\text{exp})^{+0.014}_{-0.015}(\text{th}) \leftrightarrow \gamma \\ &= (65.7^{+17.3}_{-20.7}(\text{exp})^{+8.9}_{-9.2}(\text{th}))^\circ. \end{aligned} \tag{67}$$

These numbers compare well with the Belle result [40] from tree-level processes, $\gamma = (53 \pm 20)^\circ$, quoted in

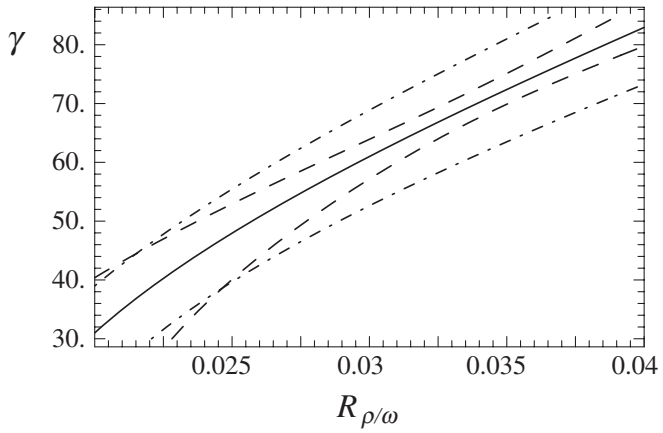

FIG. 5. The UT angle γ as a function of $R_{\rho/\omega}$ in the γ set of CKM parameters. Solid lines: central values of input parameters. Dash-dotted lines: theoretical uncertainty induced by $\xi_\rho = 1.17 \pm 0.09$. Dashed lines: other theoretical uncertainties.

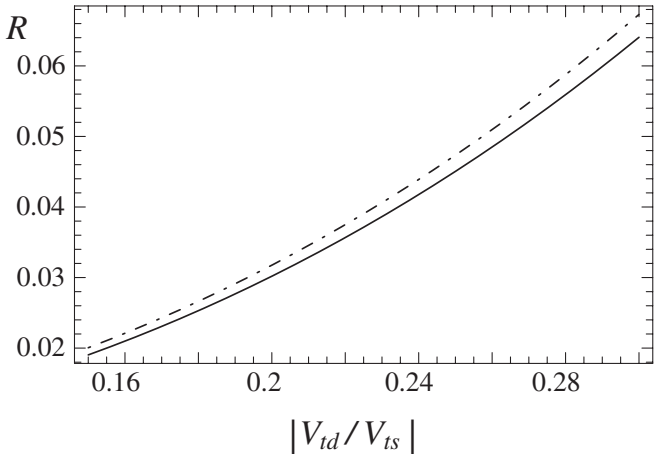

FIG. 6. Central values of $R_{\rho/\omega}$ (solid line) and R_ρ (dash-dotted line) as a function of $|V_{td}/V_{ts}|$.

TABLE XI. Central values and uncertainties of $|V_{td}/V_{ts}|$ and γ extracted from representative values of $R_{\rho/\omega}$, Eq. (63). Δ_{ξ_ρ} is the uncertainty induced by ξ_ρ, Eq. (55), and $\Delta_{\text{other th}}$ is that by other input parameters, including ξ_ω and $|V_{ub}|$.

$R_{\rho/\omega}$	$\lvert V_{td}/V_{ts}\rvert$	Δ_{ξ_ρ}	$\Delta_{\text{other th}}$	γ	Δ_{ξ_ρ}	$\Delta_{\text{other th}}$
0.026	0.183	± 0.012	± 0.007	50.8	$^{+7.5}_{-8.2}$	± 5.8
0.028	0.191	$^{+0.012}_{-0.013}$	± 0.006	56.0	$^{+7.7}_{-8.3}$	± 4.7
0.030	0.199	± 0.013	± 0.006	61.0	$^{+7.9}_{-8.4}$	± 4.0
0.032	0.207	$^{+0.013}_{-0.014}$	± 0.006	65.7	$^{+8.1}_{-8.5}$	± 3.6
0.034	0.214	± 0.014	± 0.006	70.2	$^{+8.4}_{-8.8}$	± 3.5
0.036	0.221	$^{+0.014}_{-0.015}$	± 0.006	74.5	$^{+8.8}_{-9.0}$	± 3.7

TABLE XII. Ditto for R_ρ. Δ_{ξ_ρ} is larger than in Table XI because of the increased weight of $B \to \rho\gamma$ in the isospin average; $\Delta_{\text{other th}}$ is smaller because ξ_ω does not enter.

R_ρ	$\lvert V_{td}/V_{ts}\rvert$	Δ_{ξ_ρ}	$\Delta_{\text{other th}}$	γ	Δ_{ξ_ρ}	$\Delta_{\text{other th}}$
0.028	0.186	± 0.016	± 0.005	52.4	$^{+9.9}_{-10.3}$	± 5.0
0.030	0.193	± 0.016	± 0.005	57.4	$^{+10.2}_{-10.3}$	± 3.9
0.032	0.201	± 0.017	± 0.005	62.0	± 10.5	± 3.1
0.034	0.208	± 0.017	± 0.004	66.4	$^{+10.8}_{-10.7}$	± 2.7
0.036	0.215	± 0.018	± 0.004	70.7	$^{+11.3}_{-11.0}$	± 2.5

Table III, and with results from global fits [30]. We also would like to point out that the above determination of γ is actually a determination of $\cos\gamma$, via Eq. (66), and implies, in principle, a twofold degeneracy $\gamma \leftrightarrow 2\pi - \gamma$. This is in contrast to the determination from $B \to D^{(*)}K^{(*)}$ in [40], which carries a twofold degeneracy $\gamma \leftrightarrow \pi + \gamma$. Obviously these two determinations taken together remove the degeneracy and select $\gamma \approx 55^\circ < 180^\circ$. If $\gamma \approx 55^\circ + 180^\circ$ instead, one would have $|V_{td}/V_{ts}| \approx 0.29$ from (66), which is definitely ruled out by data. Hence, the result (67) confirms the SM interpretation of γ from the tree-level CP asymmetries in $B \to D^{(*)}K^{(*)}$.

We would like to close this subsection by making explicit the dependence of the three $B \to (\rho, \omega)\gamma$ branching ratios on γ. In Fig. 7 we plot these branching ratios, for central values of the input parameters, as functions of γ. We also indicate the present experimental results from *BABAR* [4], Table I, within their 1σ uncertainty.

B. Isospin asymmetries

The asymmetries are given by

$$A(\rho, \omega) = \frac{\bar\Gamma(B^0 \to \omega\gamma)}{\bar\Gamma(B^0 \to \rho^0\gamma)} - 1, \tag{68}$$

$$A_I(\rho) = \frac{2\bar\Gamma(\bar B^0 \to \rho^0\gamma)}{\bar\Gamma(\bar B^\pm \to \rho^\pm\gamma)} - 1, \tag{69}$$

$$A_I(K^*) = \frac{\bar\Gamma(\bar B^0 \to K^{*0}\gamma) - \bar\Gamma(B^\pm \to K^{*\pm}\gamma)}{\bar\Gamma(\bar B^0 \to K^{*0}\gamma) + \bar\Gamma(B^\pm \to K^{*\pm}\gamma)}; \tag{70}$$

the partial decay rates are CP averaged; $A_I(\rho)$, $A_I(K^*)$ are isospin asymmetries.

Let us first discuss $A(\rho, \omega)$ and $A_I(\rho)$ which are relevant for the experimental determination of $\bar{\mathcal{B}}(B \to (\rho, \omega)\gamma)$, which in turn is used for the determination of $|V_{td}/V_{ts}|$ (or γ); see Sec. V A. The present experimental statistics for

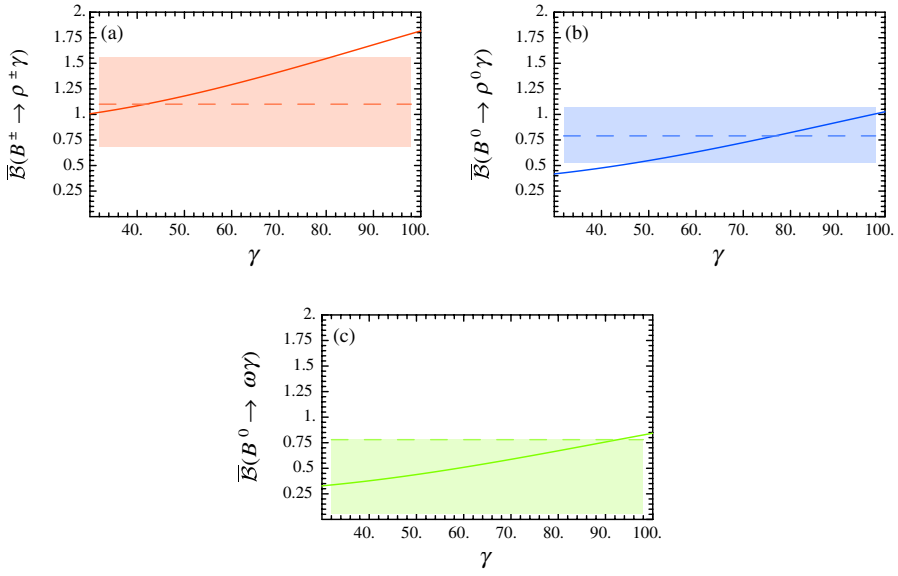

FIG. 7 (color online). CP-averaged branching ratios of $B \to (\rho, \omega)\gamma$ as a function of γ, using the effective form factors and central values of other input parameters. (a): $B^\pm \to \rho^\pm\gamma$; (b): $B^0 \to \rho^0\gamma$; (c): $B^0 \to \omega\gamma$. The boxes indicate the 1σ experimental results from *BABAR* [4], Table I. Note that the resulting value of γ from the average of all three channels is $\gamma = (61.0^{+13.5}_{-16.0}(\text{exp})^{+8.9}_{-9.2})^\circ$, Eq. (67).

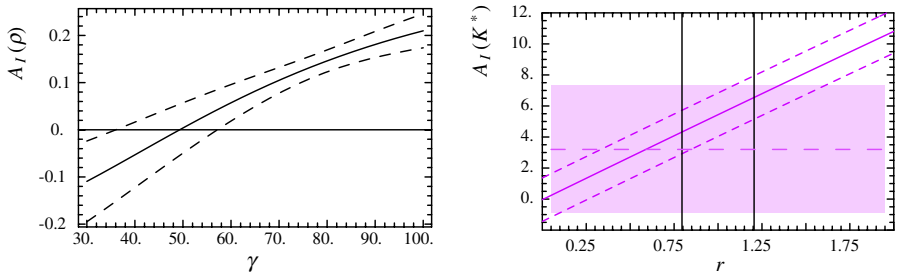

FIG. 8 (color online). Left panel: isospin asymmetry $A_I(\rho)$, Eq. (69), as a function of the UT angle γ. Solid line: central values of input parameters; dashed lines: theoretical uncertainty. Right panel: $A_I(K^*)$, Eq. (70), in percent, as a function of the ratio $r \equiv a_6/a_6^{\rm SM}$ of the combination of penguin Wilson coefficients $a_6 \equiv C_6 + C_5/3$. Solid line: central value of input parameters; dashed lines: theoretical uncertainty. The box indicates the present experimental uncertainty and the straight black lines the theory uncertainty in r.

TABLE XIII. Isospin asymmetry $A_I(\rho)$, Eq. (69), for different values of γ.

γ	40°	50°	60°	70°
$A_I(\rho)$	$-(5.3 \pm 6.9)\%$	$(0.4 \pm 5.3)\%$	$(5.7 \pm 3.9)\%$	$(10.5 \pm 2.7)\%$

$b \to d\gamma$ transitions is rather low, so the experimental value of $\bar{\mathcal{B}}(B \to (\rho, \omega)\gamma)$ is obtained under the explicit assumption of perfect symmetry, i.e. $\bar{\Gamma}(B^\pm \to \rho^\pm\gamma) = 2\bar{\Gamma}(B^0 \to \rho^0\gamma) = 2\bar{\Gamma}(B^0 \to \omega\gamma)$. In reality, the symmetry between ρ^0 and ω is broken by different values of the form factors, and isospin symmetry between neutral and charged ρ is broken by photon emission from the spectator quark, the dominant mechanism of which is WA, as discussed in Sec. III. From the formulas for individual branching ratios, Eq. (53), and the various contributions to the factorization coefficients $a^U_{7L(R)}$ collected in Secs. II, III, and IV, we find

$$A(\rho, \omega) = -0.20 \pm 0.09(\text{th}). \tag{71}$$

The uncertainty is dominated by that of the form factor ratio $T_1^{B\to\omega}(0)/T_1^{B\to\rho}(0) = 0.90 \pm 0.05$.[5] The dependence on all other input parameters is marginal. $A_I(\rho)$, on the other hand, is very sensitive to γ, whereas the form factors drop out. It is driven by the WA contribution and, in the QCDF framework, vanishes if WA is set to zero. In Fig. 8(a) we plot $A_I(\rho)$ as a function of γ, including the theoretical uncertainties. As suggested by the findings of Ref. [50], these results are not expected to change considerably upon inclusion of the nonfactorizable radiative corrections of Fig. 2(c). In Table XIII, we give the corresponding results for several values of γ, together with the theoretical uncertainty. Our result agrees very well with that obtained by the *BABAR* Collaboration: $A_I(\rho)_{BABAR} = 0.56 \pm 0.66$ [4].

[5]Note that this result is dominated by the ratio of decay constants given in Table III and discussed in the Appendix. The experimental results entering these averages have a large spread which may cast a shadow of doubt on the averaged final branching ratios for $(\rho^0, \omega) \to e^+e^-$ quoted by PDG [28].

$A_I(K^*)$ was first discussed in Ref. [20], including power-suppressed $O(\alpha_s)$ corrections which unfortunately violate QCDF, i.e. are divergent. It is for this reason that we decide to drop these corrections and include only leading-order terms in α_s. We then find

$$\begin{aligned} A_I(K^*) &= (5.4 \pm 1.0(\mu) \pm 0.6(\text{NLO} \\ &\quad \leftrightarrow \text{LO}) \pm 0.6(f_B) \pm 0.6(\text{other}))\% \\ &= (5.4 \pm 1.4)\%, \end{aligned} \tag{72}$$

where NLO $\leftrightarrow$ LO denotes the uncertainty induced by switching from NLO to LO accuracy in the Wilson coefficients and "other" summarizes all other sources of theoretical uncertainty. As can be inferred from the entries in Table I, the present experimental result is $A_I(K^*)_{\rm exp} = (3.2 \pm 4.1)\%$. In Ref. [20], Kagan and Neubert pointed out that $A_I(K^*)$ is very sensitive to the values of the Wilson coefficients $C_{5,6}^{\rm BBL}$ in the combination $a_6 \equiv C_5^{\rm BBL} + C_6^{\rm BBL}/3$. In the SM, varying the renormalization scale as $\mu = m_b(m_b) \pm 1$ GeV and switching between LO and NLO accuracy for the Wilson coefficients, one has $a_6 = -0.039 \pm 0.008$, which actually induces the bulk of the uncertainty in (72). In Fig. 8(b) we plot $A_I(K^*)$ as a function of $a_6/a_6^{\rm SM}$, with $a_6^{\rm SM} = -0.039$. The figure clearly indicates that, although there is presently no discrepancy between theoretical prediction and experimental result, a reduction of the experimental uncertainty of $A_I(K^*)$ may well reveal some footprints of NP in this observable.

C. *CP* asymmetries

The time-dependent *CP* asymmetry in $\bar{B}^0 \to V^0\gamma$ is given by

$$A_{CP}(t) = \frac{\Gamma(\bar{B}^0(t) \to V\gamma) - \Gamma(B^0(t) \to \bar{V}\gamma)}{\Gamma(\bar{B}^0(t) \to V\gamma) + \Gamma(B^0(t) \to \bar{V}\gamma)} = S(V\gamma)\sin(\Delta m_B t) - C(V\gamma)\cos(\Delta m_B t), \quad (73)$$

where we have neglected the width difference $\Delta\Gamma$ of the two neutral B mesons. This approximation is well justified for B_d, but less so for B_s. Although the above formula can easily be adapted to nonzero $\Delta\Gamma_s$, we refrain from doing so: the whole point in calculating the CP asymmetry is not so much to give precise predictions for S and C, but rather to exclude the possibility of large corrections to the naive expectation $S \sim m_D/m_b$. With this is mind, small corrections from a nonzero $\Delta\Gamma_s$ are irrelevant.

Let us briefly recall the reason for the expected smallness of S. In the process $b \to D\gamma$, in the SM, the emitted photon is predominantly left-handed in b and right-handed in $\bar{b}$ decays. This is due to the fact that the dominant contribution to the amplitude comes from the chiral-odd dipole operator Q_7, Eq. (4). As only left-handed quarks participate in the weak interaction, an effective operator of this type necessitates, in the SM, a helicity flip on one of the external quark lines, which results in a factor m_b (and a left-handed photon) in $b_R \to D_L\gamma_L$ and a factor m_D (and a right-handed photon) in $b_L \to D_R\gamma_R$. Hence, the emission of right-handed photons is suppressed by a factor m_D/m_b, which leads to the QCDF prediction (13) for a_{7R}^U.

The interesting point is not the smallness of the CP asymmetry *per se*, but the fact that the helicity suppression can easily be alleviated in a large number of NP scenarios where the spin flip occurs on an internal line, resulting in a factor m_i/m_b instead of m_D/m_b. A prime example is left-right symmetric models [61], whose impact on the photon polarization was discussed in Refs. [16–18]. These models also come in a supersymmetric version whose effect on $b \to s\gamma$ was investigated in Ref. [62]. Supersymmetry with no left-right symmetry can also provide large contributions to $b \to D\gamma_R$; see Ref. [63] for recent studies. Other potential sources of large effects are warped extra dimensions [64] or anomalous right-handed top couplings [65]. Unless the amplitude for $b \to D\gamma_R$ is of the same order as the SM prediction for $b \to D\gamma_L$, or the enhancement of $b \to D\gamma_R$ goes along with a suppression of $b \to D\gamma_L$, the impact on the branching ratio is small, as the two helicity amplitudes add incoherently. This implies there can be a substantial contribution of NP to $b \to D\gamma$ escaping detection when only branching ratios are measured.

Although the photon helicity is, in principle, an observable, it is very difficult to measure directly. It can, however, be accessed indirectly, in the time-dependent CP asymmetry in $\bar{B}^0 \to V\gamma$, which relies on the interference of both left- and right-helicity amplitudes and vanishes if one of them is absent. In terms of the left- and right-handed photon amplitudes of Eq. (5), one has

$$S(V\gamma) = \frac{2\,\mathrm{Im}(\frac{q}{p}(\mathcal{A}_L^*\bar{\mathcal{A}}_L + \mathcal{A}_R^*\bar{\mathcal{A}}_R))}{|\mathcal{A}_L|^2 + |\mathcal{A}_R|^2 + |\bar{\mathcal{A}}_L|^2 + |\bar{\mathcal{A}}_R|^2}, \qquad C(V\gamma) = \frac{|\mathcal{A}_L|^2 + |\mathcal{A}_R|^2 - |\bar{\mathcal{A}}_L|^2 - |\bar{\mathcal{A}}_R|^2}{|\mathcal{A}_L|^2 + |\mathcal{A}_R|^2 + |\bar{\mathcal{A}}_L|^2 + |\bar{\mathcal{A}}_R|^2}. \quad (74)$$

Here q/p is given in terms of the B_q^0-$\bar{B}_q^0$ mixing matrix M_{12}, in the standard convention for the parametrization of the CKM matrix, by

$$\frac{q}{p} = \sqrt{\frac{M_{12}^*}{M_{12}}} = e^{-i\phi_q}$$

with, in the Wolfenstein parametrization of the CKM matrix,

$$\phi_d \equiv \arg[(V_{td}^* V_{tb})^2] = 2\beta, \qquad \phi_s \equiv \arg[(V_{ts}^* V_{tb})^2] = -2\lambda\left|\frac{V_{ub}}{V_{cb}}\right|\sin\gamma. \quad (75)$$

This method of accessing the right-handed photon amplitude via $S(V\gamma)$ was first suggested in Ref. [16] and later discussed in more detail in Refs. [17,18]. The direct CP asymmetry $C(V\gamma)$ is less sensitive to $\bar{\mathcal{A}}_R$, but very sensitive to the strong phase of $\bar{\mathcal{A}}_L$ and vanishes if the radiative corrections to $a_{7L}^{U,\mathrm{QCDF}}$, Eq. (11), are neglected. As the accuracy of the prediction of strong phases in QCDF is subject to discussion, and in any case $C(V\gamma)$ is less sensitive to NP than $S(V\gamma)$, we shall not consider direct CP asymmetries in this paper. $S(V\gamma)$ is rather special in the sense that usually NP modifies the SM predictions for time-dependent CP asymmetries by affecting the mixing phase (as in $B_s \to J/\psi\phi$; see for instance Ref. [66]), introducing new weak phases or moderately changing the size of the decay amplitudes which, in the absence of precise calculational tools, makes it difficult to trace its impact. In contrast, the time-dependent CP asymmetry in $\bar{B}^0 \to V\gamma$ is very small in the SM, irrespective of hadronic uncertainties, and NP manifests itself by relieving this suppression. The smallness of the asymmetry in the SM, and the possibility of large effects from NP, makes the asymmetry one of the prime candidates for a so-called ''null test'' of the SM, as recently advertised in Ref. [67].

The fly in the ointment, however, is that, in addition to the helicity-suppressed contribution from Q_7, $\bar{\mathcal{A}}_R$ also receives contributions from the parton process $b \to D\gamma g$, which come without a helicity-suppression factor [17,18]. These contributions are dominated by soft-gluon and long-distance photon emission in weak annihilation and are also included in a_{7R}^U, Eq. (9). In Ref. [18] it was inferred from a dimensional estimate that these contributions could be as large as $\sim$10%, but a recent explicit calculation of the contribution of Q_2^c to $S(K^*\gamma)$ has shown that their true size is much smaller [19]. In this paper, we extend the calculation of [19] to all $\bar{B}^0 \to V^0\gamma$ channels and include the effects from all four-quark operators in the effective

Hamiltonian (2) and also the contribution from weak annihilation.

With $\mathcal{A}_{L,R}$ and $\bar{\mathcal{A}}_{L,R}$ as given in (6) we can calculate S directly from (74) and obtain, making explicit the contributions from different sources,[6]

$$\begin{aligned} S(\rho\gamma) &= (\underbrace{0.01}_{m_D/m_b} + \underbrace{0.02}_{\text{LD WA}} + \underbrace{0.20}_{\text{soft } g} \pm 1.6)\% \\ &= (0.2 \pm 1.6)\%, \\ S(\omega\gamma) &= (0.01 - 0.08 + 0.22 \pm 1.7)\% = (0.1 \pm 1.7)\%, \\ S(K^*\gamma) &= -(2.9 - 0 + 0.6 \pm 1.6)\% = -(2.3 \pm 1.6)\%, \\ S(\bar{K}^*\gamma) &= (0.12 + 0.03 + 0.11 \pm 1.3)\% = (0.3 \pm 1.3)\%, \\ S(\phi\gamma) &= (0 + 0 + 5.3 \pm 8.2) \times 10^{-2}\% = (0.1 \pm 0.1)\%. \end{aligned} \tag{76}$$

Including only the helicity-suppressed contribution, one expects, for $B \to K^*\gamma$, neglecting the doubly Cabibbo-suppressed amplitude in $\lambda_u^{(s)}$, see Eq. (2),

$$S(K^*\gamma)|_{\text{no soft gluons}} = -2\frac{m_s}{m_b}\sin\phi_d \approx -2.7\%. \tag{77}$$

For $B_s \to \phi\gamma$, one expects the CP asymmetry to vanish if the decay amplitude is proportional to $\lambda_t^{(s)}$, which, at tree level, precludes any contributions of type $\sin(\phi_s)m_s/m_b$ and also any contribution from WA.[7]

The actual results in (76) disagree with the above expectations because of the contributions from soft-gluon emission, which enter a_{7R}^U, and, for $S(\phi\gamma)$, because the soft-gluon emission from quark loops is different for u and c loops (see Sec. IV), so that $a_{7R}^c \neq a_{7R}^u$ and hence $\bar{\mathcal{A}}_R$ ($\mathcal{A}_L$) is not proportional to $\lambda_t^{(s)}$ ($(\lambda_t^{(s)})^*$). Note that a substantial enhancement of $S(\phi\gamma)$ by NP requires not only an enhancement of $|\bar{\mathcal{A}}_R|$ (and $|\mathcal{A}_L|$), but also the presence of a large phase in (74); this could be either a large B_s mixing phase which will also manifest itself in a sizable CP violation in, for instance, $B_s \to J/\psi\phi$ (see Ref. [66]), or it could be a new weak phase in $\bar{\mathcal{A}}_R$ (and $\mathcal{A}_L$), or it could be a nonzero strong phase in one of the $a_{7R}^{c,u}$ coefficients. Based on the calculation in Sec. IV B we do not see much scope for a large phase in a_{7R}^u (whose contribution is, in addition, doubly Cabibbo suppressed), but the situation could be different for $a_{7R}^{c,\text{soft}}$, where we only included the leading-order term in a $1/m_c$ expansion, which does not carry a complex phase; see Sec. IV A. It is not excluded that a resummation of higher-order terms in this expansion will generate a non-negligible strong phase—which is not really relevant for our results in Eq. (76), but could be relevant for the interpretation of any NP to be found in that observable. For $S(K^*\gamma)$, on the other hand, no new phases are required, and any enhancement of $|\bar{\mathcal{A}}_R|$ (and $|\mathcal{A}_L|$) by NP will result in a larger value of $S(K^*\gamma)$.

For all S except $S(K^*\gamma)$, the uncertainty is entirely dominated by that of the soft-gluon emission terms $l_{u,c} - \tilde{l}_{u,c}$, whose uncertainties we have doubled with respect to those given in Sec. IV. The smallness of $S((\rho, \omega)\gamma)$ is due to the fact that the helicity factor is given by m_d/m_b (we use $m_{u,d}/m_s = 1/24.4$ from chiral perturbation theory). For $\bar{K}^*$, the suppression from the small mixing angle is relieved by the fact that both weak amplitudes in $\lambda_U^{(d)}$ contribute, with different strength, so that the CP asymmetry is comparable with that of ρ and ω. Despite the generous uncertainties, it is obvious that none of these CP symmetries is larger than 4% in the SM, which makes these observables very interesting for NP searches. The present experimental result from the B factories, $S(K^*\gamma) = -0.28 \pm 0.26$ [6], certainly encourages the hope that NP may manifest itself in that observable. While a measurement of the $b \to d$ CP asymmetries is probably very difficult even at a superflavor factory, $S(K^*\gamma)$ is a promising observable for B factories [24], but not for the LHC.[8] $B_s \to \phi(\to K^+K^-)\gamma$, on the other hand, will be studied in detail at the LHC, and, in particular, at LHCb, and any largely enhanced value of $S(\phi\gamma)$ will be measured within the first years of running.

VI. SUMMARY AND CONCLUSIONS

In this paper we have presented a comprehensive study of the observables in $B \to V\gamma$ decays, namely, branching ratios, isospin and CP asymmetries, for all B_s and $B_{u,d}$ transitions,[9] including the most recent results on form factors from QCD sum rules on the light-cone and hadronic parameters describing twist-2 and twist-3 two- and three-particle light-cone distribution amplitudes of vector mesons. Our study is based on QCD factorization [9–14], but goes beyond it by including power-suppressed nonfactorizable corrections from long-distance photon emission and soft-gluon emission from quark loops which are also calculated from light-cone sum rules. In Sec. IV B we have devised a method for calculating such soft-gluon emission

[6]These results are obtained using LO Wilson coefficients. The difference between LO and NLO results is marginal.

[7]This is because the mixing angle ϕ_s is given by $\arg[(\lambda_t^{(s)})^2]$, Eq. (75), and the interference of amplitudes in (74) also yields a factor $(\lambda_t^{(s)})^2$, if the individual amplitudes are proportional to $\lambda_t^{(s)}$ or $(\lambda_t^{(s)})^*$, respectively; this is indeed the case for the helicity-suppressed term m_s/m_b induced by the operator Q_7, Eq. (4), and the WA contributions to $a_{7R}^U(\phi)$, Eqs. (15) and (20), so that the phases cancel in (74).

[8]K^* has to be traced via its decay into a CP eigenstate, i.e. $K_S\pi^0$. Neutrals in the final state are not really LHC's favorites.

[9]We have not included pure annihilation decays, for instance, $B_d \to \phi\gamma$, as their SM branching ratios are tiny, $O(10^{-11})$, and sensitive to higher-order effects in the electromagnetic interaction, which are not considered in this paper, but are, for instance, in Ref. [68].

from a light-quark loop for an on-shell photon, building on the calculation of related effects in $B \to \pi\pi$ [58]. The main idea is to calculate the loop for an off-shell photon and then use a dispersion representation to relate it to the on-shell amplitude. For phenomenology, light-quark loops are only relevant for $b \to d$ transitions, as otherwise they are Cabibbo suppressed or come with small Wilson coefficients. Our estimates may be of interest also for inclusive $b \to d\gamma$ transitions, where an interplay between exclusive and inclusive effects could take place similar to that for $b \to s\gamma$ [55–57].

Our main results are given in Sec. V. We find that the theoretical uncertainty of the branching ratios gets reduced by exploiting the fact that ratios of form factors from QCD sum rules on the light cone are known with better accuracy than the form factors themselves. This allows us to predict the branching ratios of all $B \to V\gamma$ transitions with $\sim$20% theoretical uncertainty (except for $B_s \to \phi\gamma$ which comes with a $\sim$30% uncertainty), based on the experimental input from $B \to K^*\gamma$. The effect of power corrections beyond QCD factorization is non-negligible for all decay channels, although in some channels the net corrections nearly cancel. We have determined $|V_{td}/V_{ts}|$ and, equivalently, γ, from the most recent *BABAR* [4] and Belle [5] results for $\bar{\mathcal{B}}(B \to (\rho, \omega)\gamma)/\bar{\mathcal{B}}(B \to K^*\gamma)$ as

$$\begin{aligned} \textit{BABAR}: \quad \left|\frac{V_{td}}{V_{ts}}\right| &= 0.199^{+0.022}_{-0.025}(\text{exp}) \pm 0.014(\text{th}) \leftrightarrow \gamma \\ &= (61.0^{+13.5}_{-16.0}(\text{exp})^{+8.9}_{-9.3}(\text{th}))^\circ, \\ \text{Belle}: \quad \left|\frac{V_{td}}{V_{ts}}\right| &= 0.207^{+0.028}_{-0.033}(\text{exp})^{+0.014}_{-0.015}(\text{th}) \leftrightarrow \gamma \\ &= (65.7^{+17.3}_{-20.7}(\text{exp})^{+8.9}_{-9.2}(\text{th}))^\circ. \end{aligned}$$

As the relation (66) between $|V_{td}/V_{ts}|$ and γ relies on $\cos\gamma$, these results have a twofold degeneracy $\gamma \leftrightarrow -\gamma$. Taken together with the tree-level CP asymmetries in $B \to D^{(*)}K^{(*)}$, for instance, $\gamma = (53 \pm 20)^\circ$ from Belle [40], which comes with the discrete ambiguity $\gamma \leftrightarrow \gamma + \pi$, our result removes the ambiguity and confirms that $\gamma < 180^\circ$ as predicted in the SM.

As for the isospin asymmetries, we find a nonzero asymmetry for the ρ^0 and ω channels which are driven by the difference of the corresponding form factors. The asymmetry between the neutral and the charged ρ channels, on the other hand, is very sensitive to γ, neglected radiative corrections, and hadronic input parameters, which precludes a precise statement about its size. The isospin asymmetry in $B \to K^*\gamma$ depends only mildly on the input parameters, but is sensitive to the contribution of the penguin operators $Q_{5,6}$. The sign of the asymmetry is predicted unambiguously. Although the present experimental uncertainty of the asymmetry is too large to allow any definite conclusion, any reduction could be translated into a constraint on NP contributions to the Wilson coefficients of these operators.

The time-dependent CP asymmetry $S(V\gamma)$ in $\bar{B}^0 \to V^0\gamma$ is sensitive to the photon polarization amplitudes and is power suppressed in the SM. The contribution of Q_7 is helicity suppressed; the contributions of other operators enter via the parton process $b \to D\gamma g$ with no helicity suppression, but are also found to be small. The largest CP asymmetry $\approx -2\%$ is expected for $B \to K^*\gamma$, whereas all other CP asymmetries are below the 1% level. Any value significantly different from zero, measured either at the LHC or a future flavor factory, will constitute an unequivocal signal for NP with nonstandard flavor-changing interactions.

We also would like to discuss other results for $B \to V\gamma$ available in the literature. Obviously, there are earlier results from SCET [8] and QCD factorization, Refs. [11–14], with which we agree apart from the effects of the new nonfactorizable contributions calculated in this paper and/or updated hadronic input. A variant of QCD factorization has been advocated and pursued by Ali and Parkhomenko (AP) [9,10]. Another approach is that of perturbative QCD factorization (pQCD), which has been applied to $B \to V\gamma$ in Ref. [15]. Most observables discussed in this paper, branching ratios, isospin, and CP asymmetries, have been calculated in both approaches, for $B \to (K^*, \rho, \omega)\gamma$, and we shall compare the corresponding results to ours in turn. As for the branching ratios, it is evident from Eq. (53) that the predictions depend primarily on the form factor T_1 and only to a lesser extent on the specific implementation of QCD factorization. For this reason, as AP use the same form factors as we do, namely, our predictions from QCD sum rules on the light cone [36], the results in their latest update, Ref. [10], are very close to ours. The branching ratios obtained in pQCD, on the other hand, are by more than a factor of 2 larger than ours. This discrepancy is very likely to be caused by larger values of their form factors, calculated within the same formalism; a more detailed comparison is, however, difficult because Ref. [15] does not give any explicit numbers for the T_1. Turning to isospin asymmetries, AP obtain approximately the same asymmetry $A(\rho, \omega)$, Eq. (71), between ρ^0 and ω as we do, for the same reason as above. The isospin asymmetry between the neutral and the charged ρ, Eq. (69), is more delicate, driven by weak annihilation contributions and very sensitive to the angle γ; see Table XIII. Our value, $(5.7 \pm 3.9)\%$ for $\gamma = 60^\circ$, disagrees with that given by AP, $A_I(\rho) = -(2.8 \pm 2.0)\%$ for the same angle. A likely reason is the smaller size of the weak annihilation amplitude obtained in Ref. [51], on which AP rely for that contribution, as compared to the QCD factorization result. Indeed, reducing the size of the weak annihilation contribution in the $B \to V\gamma$ amplitude, our results move closer to those of AP. Reference [15], on the other hand, obtains $A_I(\rho) = (5.7 \pm 6.0)\%$ for $\gamma \approx 60^\circ$, which coincides with our result, but comes with a larger uncertainty. As for the isospin asymmetry in the K^* system, Eq. (70), we obtain a slightly lower

value than Kagan and Neubert, Ref. [20], which is mainly due to their lower value $\lambda_{B_d} = 0.35$ GeV, compared to 0.51 GeV used by us; see Table III. In the pQCD approach, the quoted asymmetry is about half of ours, but comes with a similar relative uncertainty [15], so that we agree within errors. Concerning, finally, the time-dependent CP asymmetry $S(K^*\gamma)$ in (76), we find approximate numerical agreement with Ref. [15], where the quark loops were modeled by intermediate vector states. As emphasized earlier, the exact size of the quark-loop contributions in this channel is not crucial since it is small compared to the leading term in $m_s/m_b \sin(2\beta)$, Eq. (77). The CP asymmetries $S(\rho\gamma)$ and $S(\omega\gamma)$ were also calculated by AP, but unfortunately their formulas miss the very crucial point that in $B \to V\gamma$ one has to deal with two physically distinguishable final states, namely, $V_L\gamma_R$ and $V_R\gamma_L$, whose amplitudes must be added incoherently, not coherently as done in Refs. [9,10]. We therefore refrain from a direct comparison with their results.

As for the relevance of our results for NP searches, the time-dependent CP asymmetries are the cleanest observables since they are very small in the SM and constitute "quasi null tests" of the SM [67], in the sense that any measurement of a significantly nonzero value of these observables will be an unambiguous signal of NP. For K^*, the asymmetry has already been measured, but is compatible with zero within errors. The asymmetry in $B_s \to \phi\gamma$ is a very promising observable for the LHCb. Also, the isospin asymmetry $A_I(K^*)$, Eq. (70), is very interesting for NP searches, and would become even more interesting upon completion of the NLO calculation started by Kagan and Neubert, Ref. [20], by including, in particular, the radiative corrections to the annihilation contribution shown in Fig. 1, with the photon emitted from the final-state quark lines. In contrast, neither the isospin asymmetry between ρ^0 and $\rho^\pm$ nor the asymmetry between ρ^0 and ω are likely to be sensitive to NP. As for the branching ratios, we have, motivated by the inclusive $B \to X_s\gamma$ result, assumed no significant NP effects in $B \to K^*\gamma$, and as long as there is no breakthrough in the calculation of the absolute values of form factors, any moderate NP effects in the branching ratios are likely to be obscured by the uncertainties.

In summary, we feel that exclusive $b \to (s, d)\gamma$ transitions have a massive discovery potential for NP and envisage a great future at the LHC, which may be surpassed only by that of $b \to (s, d)\mu^+\mu^-$ decays.

ACKNOWLEDGMENTS

R. Z. is grateful to Nikolai Uraltsev for discussions on nonperturbative matrix elements. G. W. J. was supported in part by a grant from the UK PPARC. This work was supported in part by the EU networks Contract No. MRTN-CT-2006-035482, FLAVIANET, and No. MRTN-CT-2006-035505, HEPTOOLS.

Note added.— After completion of the calculations presented in this paper, Ref. [46] appeared which contains a lattice calculation of $T_1^{B\to K^*}(0)$ and ξ_ρ in the quenched approximation. The results are $T_1^{B\to K^*}(0) = 0.24 \pm 0.03^{+0.04}_{-0.01}$ and $\xi_\rho = 1.2 \pm 0.1$. The latter agrees with ours, Eq. (55), but comes with a slightly larger central value and uncertainty, while the former is a bit on the low side of the LCSR prediction given in Table III.

APPENDIX A: VECTOR-MESON DECAY CONSTANTS REVISITED

There are two types of decay constants for vector mesons: the vector coupling f_V, for a longitudinally polarized meson, and the tensor coupling $f_V^\perp$, for a transversely polarized meson:

$$\begin{aligned}\langle 0|\bar{q}\gamma_\mu D|V(p,e)\rangle &= e_\mu m_V f_V,\\ \langle 0|\bar{q}\sigma_{\mu\nu} D|V(p,e)\rangle_\mu &= i(e_\mu p_\nu - e_\nu p_\mu) f_V^\perp(\mu).\end{aligned} \tag{A1}$$

Note that $f_V^\perp(\mu)$ depends on the renormalization scale.

The numerical values of these couplings are essential for our calculations. Whereas the extraction of the charged mesons' vector couplings from experimental data is straightforward, that of the neutral mesons' ρ^0, ω, and ϕ is complicated by the mixing of these particles and deserves a more detailed discussion, which we will give in Appendix A 1. The tensor couplings are not accessible experimentally, but have to be determined by nonperturbative methods, for instance, QCD sum rules and lattice simulations. In Appendixes A 2 and A 3, we briefly review the most recent results from these calculations.

1. Longitudinal decay constants from experiment

a. The charged decay constants $f_{\rho^-,K^{*-}}$ from τ decays

The longitudinal decay constants of charged vector mesons can be extracted from $\tau^- \to V^-\nu_\tau$, with the measured branching ratios [28]

$$\begin{aligned}\mathcal{B}(\tau^- \to \rho^-\nu_\tau) &= (25.2 \pm 0.4) \times 10^{-2},\\ \mathcal{B}(\tau^- \to K^{*-}\nu_\tau) &= (1.29 \pm 0.05) \times 10^{-2}.\end{aligned}$$

The decay rate is given by

$$\Gamma(\tau^- \to V^-\nu_\tau) = \frac{m_\tau^3}{16\pi} G_F^2 |V_{uD}|^2 f_{V^-}^2 \left(1 - \frac{m_{V^-}^2}{m_\tau^2}\right)^2 \times \left(1 + 2\frac{m_{V^-}^2}{m_\tau^2}\right).$$

With $|V_{ud}| = 0.9738 \pm 0.0002$ and $|V_{us}| = 0.227 \pm 0.001$ [28], we get

$$\begin{aligned}f_{\rho^-} &= (210 \pm 2_{\mathcal{B}} \pm 1_{\Gamma_\tau})\ \text{MeV},\\ f_{K^{*-}} &= (220 \pm 4_{\mathcal{B}} \pm 1_{\Gamma_\tau} \pm 1_{|V_{us}|})\ \text{MeV},\end{aligned} \tag{A2}$$

where we have taken into account the uncertainties in the

branching ratios, total decay rates, and CKM matrix elements. The uncertainties of other input parameters are irrelevant and the size of neglected corrections to the decay rate in α and higher powers in $1/m_W^2$ is expected to be smaller than the total uncertainty.

b. The neutral decay constants $f_{\rho^0,\omega,\phi}$ from $V^0 \to e^+e^-$

The decay constants of ρ^0, ω, and ϕ can be extracted from the electromagnetic annihilation process $V^0 \to e^+e^-$, which is, however, complicated by the mixing of these mesons. The states of definite isospin are given by

$$|\rho_I^0\rangle = \frac{1}{\sqrt{2}}(|\bar{u}u\rangle - |\bar{d}d\rangle), \qquad |\omega_I\rangle = \frac{1}{\sqrt{2}}(|\bar{u}u\rangle + |\bar{d}d\rangle), \qquad |\phi_I\rangle = |\bar{s}s\rangle, \tag{A3}$$

where ρ has isospin 1 and ω and ϕ have isospin 0. In view of the subtleties of mixing, let us state clearly that the neutral decay constants f_{ρ^0}, f_ω, and f_ϕ shall denote the coupling of the real particles to their isospin currents, e.g. $\langle 0|\bar{s}\gamma_\mu s|\phi\rangle \equiv e_\mu m_\phi f_\phi$. ρ-ω mixing violates isospin and hence is a purely electromagnetic effect which can be parametrized as

$$|\rho\rangle \sim |\rho_I\rangle - \epsilon_{\rho\omega}|\omega_I\rangle, \qquad |\omega\rangle \sim |\omega_I\rangle + \epsilon_{\rho\omega}|\rho_I\rangle \tag{A4}$$

with $\epsilon_{\rho\omega} = \delta_{\rho\omega}/((m_\omega - i\Gamma_\omega/2)^2 - (m_\rho - i\Gamma_\rho/2)^2)$ and $\delta_{\rho\omega} = -(0.004 \pm 0.002)\ \mathrm{GeV}^2$ [69], which results in $\epsilon_{\rho\omega} = (0.036 \pm 0.018)ie^{0.15i}$; since $m_\rho \approx m_\omega$, $\epsilon_{\rho\omega}$ is almost purely imaginary. This parameter was also determined experimentally [70]. The mixing of ω and ϕ, on the other hand, is due to strong interactions:

$$|\omega\rangle \sim |\omega_I\rangle - \epsilon_{\omega\phi}|\phi_I\rangle, \qquad |\phi\rangle \sim |\phi_I\rangle + \epsilon_{\omega\phi}|\omega_I\rangle. \tag{A5}$$

The mixing parameter has been determined to be $\epsilon_{\omega\phi} = 0.045 \pm 0.01$ [71] by parametrizing the SU(3) breaking in order to match the Gell-Mann–Okubo mass relation for light mesons with the observed masses. A direct measurement of this quantity was reported in $\omega \to e^+e^-$ decays [72]. Evidently, a full description of the mixing would involve all three states, but ρ-ϕ mixing is expected to be very small because it is a second-order effect that requires both electromagnetic and strong interactions to be at work.

As the $V^0 \to e^+e^-$ transition is an electromagnetic decay process, one needs the relevant electromagnetic currents of light quarks:

$$j_\mu^{\mathrm{em}} = Q_u\bar{u}\gamma_\mu u + Q_d\bar{d}\gamma_\mu d + Q_s\bar{s}\gamma_\mu s = \frac{1}{3\sqrt{2}}(j_\mu^{I=0} + 3j_\mu^{I=1}) - \frac{1}{3}\bar{s}\gamma_\mu s; \tag{A6}$$

the isospin currents are defined as $j_\mu^{I=0/1} = \frac{1}{\sqrt{2}}(\bar{u}\gamma_\mu u \pm \bar{d}\gamma_\mu d)$. The experimental rates are [28]

$$\begin{aligned}\mathcal{B}(\rho^0 \to e^+e^-) &= (4.7 \pm 0.08) \times 10^{-5},\\ \mathcal{B}(\omega \to e^+e^-) &= (7.18 \pm 0.12) \times 10^{-5},\\ \mathcal{B}(\phi \to e^+e^-) &= (2.97 \pm 0.04) \times 10^{-5}.\end{aligned} \tag{A7}$$

The theoretical expression for the decay rate is given by

$$\Gamma(V^0 \to e^+e^-) = \frac{4\pi}{3}\frac{\alpha^2}{m_V}f_V^2 c_V, \tag{A8}$$

where the coefficients c_V in the limit of no mixing can be read off from (A3) and (A6): $c_{\rho_I^0} = (Q_u - Q_d)^2/2 = 1/2$, $c_{\omega_I} = (Q_u + Q_d)^2/2 = 1/18$, and $c_{\phi_I} = Q_s^2 = 1/9$. The effect of, for instance, ρ-ω mixing is to change c_{ρ^0} to $c_{\rho^0} = |\sqrt{c_{\rho_I^0}} - \epsilon_{\rho\omega}\sqrt{c_{\omega_I}}|^2/|1 + \epsilon_{\rho\omega}|^2$ and correspondingly for c_ω. Including the mixing effects we finally get

$$\begin{aligned}f_{\rho^0} &= (222 \pm 2_{\mathrm{Br}} \pm 1_{\Gamma_\rho})\ \mathrm{MeV},\\ f_\omega &= (187 \pm 2_{\mathrm{Br}} \pm 1_{\Gamma_\omega} \pm 4_{\omega\phi} \pm 1_{\rho\omega})\ \mathrm{MeV},\\ f_\phi &= (215 \pm 2_{\mathrm{Br}} \pm 1_{\Gamma_\phi} \pm 4_{\omega\phi})\ \mathrm{MeV},\end{aligned} \tag{A9}$$

where again the uncertainties in the other input parameters are irrelevant and the corrections to (A8) are expected to be smaller than the total uncertainty. ρ-ω mixing has a negligible effect on f_{ρ^0}, but raises f_ω by 2 to 3 MeV. ω-ϕ mixing is much more relevant and lowers f_ω by about 10 MeV and f_ϕ by about 13 MeV.

2. Decay constants from QCD sum rules

The calculation of decay constants from QCD sum rules was one of the earliest applications of this method [73]. More recent determinations include more (radiative and mass) corrections and updated values of input parameters. The most recent results were obtained in Refs. [22,37] and read

$$\begin{aligned}f_\rho &= (206 \pm 7)\ \mathrm{MeV},\\ f_\rho^\perp(1\ \mathrm{GeV}) &= (165 \pm 9)\ \mathrm{MeV},\\ f_{K^*} &= (222 \pm 8)\ \mathrm{MeV},\\ f_{K^*}^\perp(1\ \mathrm{GeV}) &= (185 \pm 10)\ \mathrm{MeV}.\end{aligned} \tag{A10}$$

Note that the determination of $f_{K^*}^\perp$ is more complicated than that of the other couplings and requires the inclusion of higher resonances in the hadronic dispersion relation [37]. The above results refer to charged mesons; isospin breaking and meson mixing are not included. For comparison with lattice results, it proves convenient to also quote the results for the ratio of couplings[10]:

[10]Including the NLO scaling factor $f_V^\perp(2\ \mathrm{GeV})/f_V^\perp(1\ \mathrm{GeV}) = 0.876$.

$$\left(\frac{f_\rho^\perp}{f_\rho^\parallel}\right)_{\rm SR}(2\ {\rm GeV}) = 0.70 \pm 0.04,$$
$$\left(\frac{f_{K^*}^\perp}{f_{K^*}^\parallel}\right)_{\rm SR}(2\ {\rm GeV}) = 0.73 \pm 0.04. \tag{A11}$$

3. Decay constants from lattice QCD

The ratio of decay constants $f_V^\perp/f_V$ has been calculated by two lattice collaborations, in the quenched approximation. Reference [74] obtains

$$\left(\frac{f_\rho^\perp}{f_\rho^\parallel}\right)_{\rm latt}(2\ {\rm GeV}) = 0.72 \pm 0.02,$$
$$\left(\frac{f_{K^*}^\perp}{f_{K^*}^\parallel}\right)_{\rm latt}(2\ {\rm GeV}) = 0.74 \pm 0.02, \tag{A12}$$
$$\left(\frac{f_\phi^\perp}{f_\phi^\parallel}\right)_{\rm latt}(2\ {\rm GeV}) = 0.76 \pm 0.01,$$

in the continuum limit, whereas Ref. [75] quotes

$$\left(\frac{f_\rho^\perp}{f_\rho^\parallel}\right)_{\rm latt}(2\ {\rm GeV}) = 0.742 \pm 0.014,$$
$$\left(\frac{f_\phi^\perp}{f_\phi^\parallel}\right)_{\rm latt}(2\ {\rm GeV}) = 0.780 \pm 0.008, \tag{A13}$$

at the finite lattice spacing $a = 0.10$ fm.

The results from both lattice collaborations are roughly in agreement. It is evident that the ratios depend only weakly on the quark masses.

4. Discussion, conclusions and results

In this paper we use the experimental results (A2) and (A9) for the longitudinal decay constants, averaging the two results for the ρ meson. For the tensor couplings of ρ and K^* we use the sum rule results (A10). For ω, we assume isospin symmetry of the ratio of decay constants and use $f_\omega^\perp(2\ {\rm GeV})/f_\omega = 0.71 \pm 0.03$, which is the average of QCD sum rule and lattice results, to obtain a value for $f_\omega^\perp$ from the measured f_ω. Finally, for ϕ we use the lattice ratio (A12), with the more conservative uncertainty ± 0.03, and the experimental value for f_ϕ. Our final results which enter Table III are

$$\begin{aligned} f_\rho &= (216 \pm 3)\ {\rm MeV}, \\ f_\rho^\perp(1\ {\rm GeV}) &= (165 \pm 9)\ {\rm MeV}, \\ f_\omega &= (187 \pm 5)\ {\rm MeV}, \\ f_\omega^\perp(1\ {\rm GeV}) &= (151 \pm 9)\ {\rm MeV}, \\ f_{K^*} &= (220 \pm 5)\ {\rm MeV}, \\ f_{K^*}^\perp(1\ {\rm GeV}) &= (185 \pm 10)\ {\rm MeV}, \\ f_\phi &= (215 \pm 5)\ {\rm MeV}, \\ f_\phi^\perp(1\ {\rm GeV}) &= (186 \pm 9)\ {\rm MeV}. \end{aligned} \tag{A14}$$

The experimental vector couplings, (A2) and (A9), come with rather small uncertainties and indicate an isospin breaking in $f_{\rho^{0,\pm}}$ of $\approx 5\%$. Is it really justified to average both results into only one decay constant for the ρ? In order to answer this question, let us have a look at the experimental information on isospin breaking in other light-meson decay constants. For the π, PDG gives $f_{\pi^\pm} = (130.7 \pm 0.4)$ MeV, whereas f_{π^0} is extracted from $\pi^0 \to \gamma\gamma$ as (130 ± 5) MeV which is perfectly compatible with $f_{\pi^\pm}$; the uncertainty is dominated by that of the π^0 lifetime [76]. A further confirmation of the smallness of isospin breaking comes from the CLEO measurements of $D^0 \to (K^-, \pi^-)e^+\nu$ and $D^+ \to (\bar{K}^0, \pi^0)e^+\nu$ [47]. These decays are sensitive to the π and K meson decay constants via the form factors, which, at least in the LCSR approach, are directly proportional to $f_{\pi,K}$; see e.g. Ref. [77]. The data for $D \to Ke\nu$ indicate that the isospin breaking of the form factor is $(3 \pm 2)\%$. Although this result also includes potential isospin breaking of both f_D and the dynamical part of the form factor, the corresponding effects are neither expected to be sizable nor to cancel each other, so that indeed for both π and K decay constants isospin breaking is smaller than 5% at 1σ. Taking this as an indication for the generic size of isospin breaking in light mesons, we conclude that a 5% difference between f_{ρ^0} and $f_{\rho^\pm}$ is not excluded, but on the large side. This implies that it is indeed appropriate to average the experimental results for neutral and charged ρ as done in (A14).

Note that the QCD sum rule results for the vector couplings, (A10), agree rather well with the experimental results, (A2) and (A9), which increases confidence in the corresponding results for the tensor couplings, particularly as the sum rule results for the ratios, (A11), also agree with those from lattice, (A12). Nevertheless there is one fact which remains somewhat puzzling, namely, the difference of nearly 20% between the ω and ρ^0 couplings from $V^0 \to e^+e^-$, which is larger than the expectation from QCD sum rules. This difference could be caused by electromagnetic corrections, different values of the up- and down-quark condensate, and differences in the continuum thresholds and Borel windows. The latter effects should not exceed the typical accuracy of sum rules themselves, which is about 10%, and the former effects are expected to be very small. On the other hand, the individual experimental

results entering the PDG averages (A7) are spread over a wide range, particularly for ω, which indicates that the uncertainties quoted in (A7) may be on the optimistic side.

There remains one subtle point to be discussed, namely, that for LCSRs for $b \to d\gamma$ transitions and ρ^0 or ω in the final state, one needs the decay constant

$$\sqrt{2}\langle 0|\bar{d}\gamma_\mu d|V^0(e)\rangle = e_\mu m_{V^0} f_{V^0}^{(d)},$$

rather than f_{V^0}. The quantity $f_{V^0}^{(d)}$ could differ from f_{V^0} through mixing with the other neutral mesons. Fortunately, ω-ϕ mixing is irrelevant because the coupling of ϕ to the down-quark current is highly suppressed, and ρ-ω mixing has a small effect because the mixing parameter is almost imaginary. The total impact of mixing is hence below the theoretical uncertainty and can safely be neglected.

[1] T. Hurth, Rev. Mod. Phys. **75**, 1159 (2003).
[2] M. Misiak *et al.*, Phys. Rev. Lett. **98**, 022002 (2007).
[3] M. Misiak and M. Steinhauser, Nucl. Phys. **B683**, 277 (2004); M. Gorbahn and U. Haisch, Nucl. Phys. **B713**, 291 (2005); M. Gorbahn, U. Haisch, and M. Misiak, Phys. Rev. Lett. **95**, 102004 (2005); M. Misiak and M. Steinhauser, Nucl. Phys. **B764**, 62 (2007).
[4] B. Aubert (*BABAR* Collaboration), hep-ex/0607099; hep-ex/0612017.
[5] K. Abe *et al.*, Phys. Rev. Lett. **96**, 221601 (2006).
[6] E. Barberio *et al.* (HFAG), hep-ex/0603003; updated results available at http://www.slac.stanford.edu/xorg/hfag/.
[7] T. Becher and M. Neubert, Phys. Rev. Lett. **98**, 022003 (2007).
[8] T. Becher, R. J. Hill, and M. Neubert, Phys. Rev. D **72**, 094017 (2005).
[9] A. Ali and A. Y. Parkhomenko, Eur. Phys. J. C **23**, 89 (2002); A. Ali, E. Lunghi, and A. Y. Parkhomenko, Phys. Lett. B **595**, 323 (2004).
[10] A. Ali and A. Parkhomenko, hep-ph/0610149.
[11] M. Beneke, T. Feldmann, and D. Seidel, Eur. Phys. J. C **41**, 173 (2005).
[12] S. W. Bosch and G. Buchalla, Nucl. Phys. **B621**, 459 (2002).
[13] S. W. Bosch, hep-ph/0208203.
[14] S. W. Bosch and G. Buchalla, J. High Energy Phys. 01 (2005) 035.
[15] Y. Y. Keum, M. Matsumori, and A. I. Sanda, Phys. Rev. D **72**, 014013 (2005); C. D. Lu, M. Matsumori, A. I. Sanda, and M. Z. Yang, Phys. Rev. D **72**, 094005 (2005); **73**, 039902(E) (2006); M. Matsumori and A. I. Sanda, Phys. Rev. D **73**, 114022 (2006).
[16] D. Atwood, M. Gronau, and A. Soni, Phys. Rev. Lett. **79**, 185 (1997).
[17] B. Grinstein, Y. Grossman, Z. Ligeti, and D. Pirjol, Phys. Rev. D **71**, 011504 (2005).
[18] B. Grinstein and D. Pirjol, Phys. Rev. D **73**, 014013 (2006).
[19] P. Ball and R. Zwicky, Phys. Lett. B **642**, 478 (2006).
[20] A. L. Kagan and M. Neubert, Phys. Lett. B **539**, 227 (2002).
[21] A. Hardmeier, E. Lunghi, D. Pirjol, and D. Wyler, Nucl. Phys. **B682**, 150 (2004); T. Feldmann and T. Hurth, J. High Energy Phys. 11 (2004) 037.
[22] P. Ball and R. Zwicky, J. High Energy Phys. 04 (2006) 046.
[23] P. Ball and E. Kou, J. High Energy Phys. 04 (2003) 029.
[24] A. G. Akeroyd *et al.* (SuperKEKB Physics Working Group), hep-ex/0406071; J. Hewett *et al.*, hep-ph/0503261.
[25] G. Buchalla, A. J. Buras, and M. E. Lautenbacher, Rev. Mod. Phys. **68**, 1125 (1996).
[26] K. G. Chetyrkin, M. Misiak, and M. Münz, Phys. Lett. B **400**, 206 (1997); **425**, 414(E) (1998).
[27] C. Greub, T. Hurth, and D. Wyler, Phys. Rev. D **54**, 3350 (1996); A. J. Buras, A. Czarnecki, M. Misiak, and J. Urban, Nucl. Phys. **B611**, 488 (2001); **B631**, 219 (2002).
[28] W. M. Yao *et al.* (Particle Data Group), J. Phys. G **33**, 1 (2006).
[29] E. Brubaker *et al.* (Tevatron Electroweak Working Group), hep-ex/0608032.
[30] J. Charles *et al.* (CKMfitter Group), Eur. Phys. J. C **41**, 1 (2005); updated results and plots available at http://ckmfitter.in2p3.fr; M. Bona *et al.* (UTfit Collaboration), J. High Energy Phys. 10 (2006) 081; updated results available at http://www.utfit.org/.
[31] P. Ball and R. Zwicky, Phys. Lett. B **625**, 225 (2005); E. Dalgic *et al.*, Phys. Rev. D **73**, 074502 (2006); P. Ball, Phys. Lett. B **644**, 38 (2007).
[32] P. Ball and V. M. Braun, Phys. Rev. D **54**, 2182 (1996).
[33] P. Ball, V. M. Braun, Y. Koike, and K. Tanaka, Nucl. Phys. **B529**, 323 (1998); P. Ball and V. M. Braun, Nucl. Phys. **B543**, 201 (1999).
[34] P. Ball and M. Boglione, Phys. Rev. D **68**, 094006 (2003).
[35] P. Ball, V. M. Braun, and A. Lenz, J. High Energy Phys. 05 (2006) 004.
[36] P. Ball and R. Zwicky, Phys. Rev. D **71**, 014029 (2005).
[37] P. Ball and R. Zwicky, Phys. Lett. B **633**, 289 (2006).
[38] P. Ball and R. Zwicky, J. High Energy Phys. 02 (2006) 034.
[39] O. Buchmüller and H. Flächer, Phys. Rev. D **73**, 073008 (2006).
[40] A. Poluektov *et al.* (Belle Collaboration), Phys. Rev. D **73**, 112009 (2006).
[41] T. Onogi, Proc. Sci., LAT2006 (2006) 017.
[42] E. Gamiz *et al.*, Phys. Rev. Lett. **94**, 011803 (2005); S. Narison, Phys. Rev. D **74**, 034013 (2006); F. Knechtli, Acta Phys. Pol. B **36**, 3377 (2005).
[43] R. Boughezal, M. Czakon, and T. Schutzmeier, Phys. Rev. D **74**, 074006 (2006).
[44] I. I. Balitsky, V. M. Braun, and A. V. Kolesnichenko, Nucl. Phys. **B312**, 509 (1989).

[45] P. Ball and G. W. Jones, hep-ph/0702100.
[46] D. Becirevic, V. Lubicz, and F. Mescia, hep-ph/0611295.
[47] R. Poling, hep-ex/0606016; Y. Gao (CLEO Collaboration), in Proceedings of ICHEP06, Moscow, 2006 (unpublished).
[48] A. Giri, Y. Grossman, A. Soffer, and J. Zupan, Phys. Rev. D **68**, 054018 (2003).
[49] B. Aubert *et al.* (*BABAR* Collaboration), hep-ex/0507101; D. Marciano (*BABAR* Collaboration), in Proceedings of ICHEP06, Moscow, 2006 (unpublished).
[50] V. Pilipp, in Proceedings of the Workshop on Flavour Dynamics, Chamonix, France, 2005 (unpublished).
[51] A. Khodjamirian, G. Stoll, and D. Wyler, Phys. Lett. B **358**, 129 (1995); A. Ali and V. M. Braun, Phys. Lett. B **359**, 223 (1995).
[52] S. Descotes-Genon and C. T. Sachrajda, Nucl. Phys. **B650**, 356 (2003); E. Lunghi, D. Pirjol, and D. Wyler, Nucl. Phys. **B649**, 349 (2003).
[53] P. Ball, V. M. Braun, and N. Kivel, Nucl. Phys. **B649**, 263 (2003).
[54] A. Khodjamirian, R. Rückl, G. Stoll, and D. Wyler, Phys. Lett. B **402**, 167 (1997).
[55] M. B. Voloshin, Phys. Lett. B **397**, 275 (1997).
[56] Z. Ligeti, L. Randall, and M. B. Wise, Phys. Lett. B **402**, 178 (1997).
[57] G. Buchalla, G. Isidori, and S. J. Rey, Nucl. Phys. **B511**, 594 (1998).
[58] A. Khodjamirian, Nucl. Phys. **B605**, 558 (2001).
[59] A. Khodjamirian, Eur. Phys. J. C **6**, 477 (1999).
[60] J. Simone, in Proceedings of Lattice 2006, Tucson, Arizona, 2006 (unpublished); A. Gray *et al.* (HPQCD Collaboration), Phys. Rev. Lett. **95**, 212001 (2005).
[61] R. N. Mohapatra and J. C. Pati, Phys. Rev. D **11**, 566 (1975); **11**, 2558 (1975); G. Senjanovic and R. N. Mohapatra, Phys. Rev. D **12**, 1502 (1975); G. Senjanovic, Nucl. Phys. **B153**, 334 (1979).
[62] M. Frank and S. Nie, Phys. Rev. D **65**, 114006 (2002).
[63] E. J. Chun, K. Hwang, and J. S. Lee, Phys. Rev. D **62**, 076006 (2000); L. L. Everett *et al.*, J. High Energy Phys. 01 (2002) 022; T. Goto *et al.*, Phys. Rev. D **70**, 035012 (2004); C. K. Chua, W. S. Hou, and M. Nagashima, Phys. Rev. Lett. **92**, 201803 (2004); W. S. Hou and M. Nagashima, hep-ph/0602124.
[64] K. Agashe, G. Perez, and A. Soni, Phys. Rev. Lett. **93**, 201804 (2004); Phys. Rev. D **71**, 016002 (2005).
[65] J. P. Lee, Phys. Rev. D **69**, 014017 (2004).
[66] P. Ball, S. Khalil, and E. Kou, Phys. Rev. D **69**, 115011 (2004); P. Ball and R. Fleischer, Eur. Phys. J. C **48**, 413 (2006).
[67] T. Gershon and A. Soni, J. Phys. G **34**, 479 (2007).
[68] Y. Li and C. D. Lu, Phys. Rev. D **74**, 097502 (2006); C. D. Lu, Y. L. Shen, and W. Wang, Chin. Phys. Lett. **23**, 2684 (2006).
[69] M. A. Shifman, A. I. Vainshtein, and V. I. Zakharov, Nucl. Phys. **B147**, 519 (1979).
[70] M. Basile *et al.*, in *Proceedings of the International Conference on "Meson Resonances and Related Electromagnetic Phenomena," Bologna, Italy, 1971* (Editrice Compositori, Bologna, 1972), p. 139.
[71] J. Sakurai, Phys. Rev. Lett. **9**, 472 (1962).
[72] D. Bollini *et al.*, Nuovo Cimento A **57**, 404 (1968).
[73] M. A. Shifman, A. I. Vainshtein, and V. I. Zakharov, Nucl. Phys. **B147**, 448 (1979).
[74] D. Becirevic *et al.*, J. High Energy Phys. 05 (2003) 007.
[75] V. M. Braun *et al.*, Phys. Rev. D **68**, 054501 (2003).
[76] M. Suzuki, review of pseudoscalar-meson decay constants in Ref. [28].
[77] P. Ball, Phys. Lett. B **641**, 50 (2006).